New Selective AT_2 Receptor Ligands Encompassing a γ-Turn Mimetic Replacing the Amino Acid Residues 4−5 of Angiotensin II Act as Agonists

Ulrika Rosenström,[†] Christian Sköld,[†] Bianca Plouffe,[‡] Hélène Beaudry,[‡] Gunnar Lindeberg,[†] Milad Botros,[§] Fred Nyberg,[§] Gunter Wolf,[∥] Anders Karlén,[†] Nicole Gallo-Payet,*[,‡] and Anders Hallberg*[,†]

Department of Medicinal Chemistry, BMC, Uppsala University, P.O. Box 574, SE-751 23 Uppsala, Sweden, Service of Endocrinology, Faculty of Medicine, University of Sherbrooke, Sherbrooke, Quebec J1H 5N4, Canada, Department of Biological Research on Drug Dependence, BMC, Uppsala University, P.O. Box 591, SE-751 24 Uppsala, Sweden, and Department of Medicine, Division of Nephrology and Osteology, University of Hamburg, University Hospital Eppendorf, Martinistrasse 52, D-20246 Hamburg, FRG

Received October 25, 2004

New benzodiazepine-based γ-turn mimetics with one or two amino acid side chains were synthesized. The γ-turn mimetics were incorporated into angiotensin II (Ang II) replacing the Val^3-Tyr^4-Ile^5 or Tyr^4-Ile^5 peptide segments. All of the resulting pseudopeptides displayed high AT_2/AT_1 receptor selectivity and exhibited AT_2 receptor affinity in the low nanomolar range. Molecular modeling was used to investigate whether the compounds binding to the AT_2 receptor could position important structural elements in common areas. A previously described benzodiazepine-based γ-turn mimetic with high affinity for the AT_2 receptor was also included in the modeling. It was found that the molecules, although being structurally quite different, could adopt the same binding mode/interaction pattern in agreement with the model hypothesis. The pseudopeptides selected for agonist studies were shown to act as AT_2 receptor agonists being able to induce outgrowth of neurite cells, stimulate $p42/p44^{mapk}$, and suppress proliferation of PC12 cells.

Introduction

The octapeptide angiotensin II (Ang II, Asp-Arg-Val-Tyr-Ile-His-Pro-Phe) mediates its biological actions by activating at least two distinct receptor subtypes, designated AT_1 and AT_2. Both receptors are seven-transmembrane G-protein coupled receptors with 32−34% sequence homology.[1,2] Most of the more well-known physiological effects of Ang II, including vasoconstriction, aldosterone release, stimulation of sympathetic transmission, and cellular growth, are generally attributed to AT_1 receptor activation.[3−5] The role of the AT_2 receptor has been less clear, largely because of its often low level of expression in adults. However, roles of the AT_2 receptor in mediating antiproliferation, cellular differentiation, programmed cell death (apoptosis), and even vasodilation have been proposed.[6−10] The AT_2 receptor is the predominant angiotensin receptor in fetal tissues but is rapidly downregulated after birth, suggesting its involvement in fetal development.[11,12] Importantly in adults it is upregulated in certain pathological conditions such as heart failure, myocardial infarction, brain lesions, vascular injury, and wound healing.[13−18] It has also been shown that activation of the AT_2 receptor in cells of neuronal origin induce neurite outgrowth and elongation, modulate neuronal exitability, and promote cellular migration in adults.[8]

The signaling pathways activated by the AT_2 receptor are still controversial. The AT_2 receptor is not coupled to any of the classical, well-established, second messengers for G-protein-coupled receptors, such as cAMP or inositol phosphatases, and its coupling to a $G_{\alpha i}$ protein, reported by several authors is not viewed in consensus (for reviews see refs 4, 8, and 19−22). However, various mediators, which could individually exert opposite effects, such as cGMP, tyrosine or serine/threonine phosphatases, and the extracellular signal regulated kinases ERK1/ERK2 ($p42/p44^{mapk}$), have been associated with the activation of the AT_2 receptor, depending on the cell types and experimental conditions used. More precisely, a sustained increase in $p42/p44^{mapk}$ activity is associated with neuronal differentiation.[23,24]

Information of the bioactive conformation of Ang II when bound to its receptors is invaluable for the understanding of the topological requirements within the peptide−receptor complex. In this context, constrained analogues are important research tools and various cyclization strategies have been employed to introduce conformational constrains in Ang II.[25−34] An important driving force for the research is to enable the conversion of peptides into more druglike compounds. Cyclization can be a powerful tool and transform peptide leads into peptidomimetic compounds.[35,36] Several models of the bioactive conformation of Ang II when interacting with the AT_1 receptor have been proposed.[32,37−44] Thus, it has been suggested by several groups that Ang II adopts a turn conformation around the Tyr^4 residue[25,26,29,30,37−39,45−47] but also extended conformations of Ang II have been considered.[48] Much less is reported on the structural requirements for AT_2

* Corresponding authors: e-mail anders.hallberg@orgfarm.uu.se, tel +46-18-4714284, fax +46-18-4714474; e-mail nicole.gallo-payet@usherbrooke.ca, tel +1-819-5645243, fax +1-819-5645292.

[†] Department of Medicinal Chemistry, Uppsala University.

[‡] Service of Endocrinology, University of Sherbrooke.

[§] Department of Biological Research on Drug Dependence, Uppsala University.

[∥] Department of Medicine, University of Hamburg.

10.1021/jm0491492 CCC: $30.25
Published on Web 05/13/2005

Chart 1

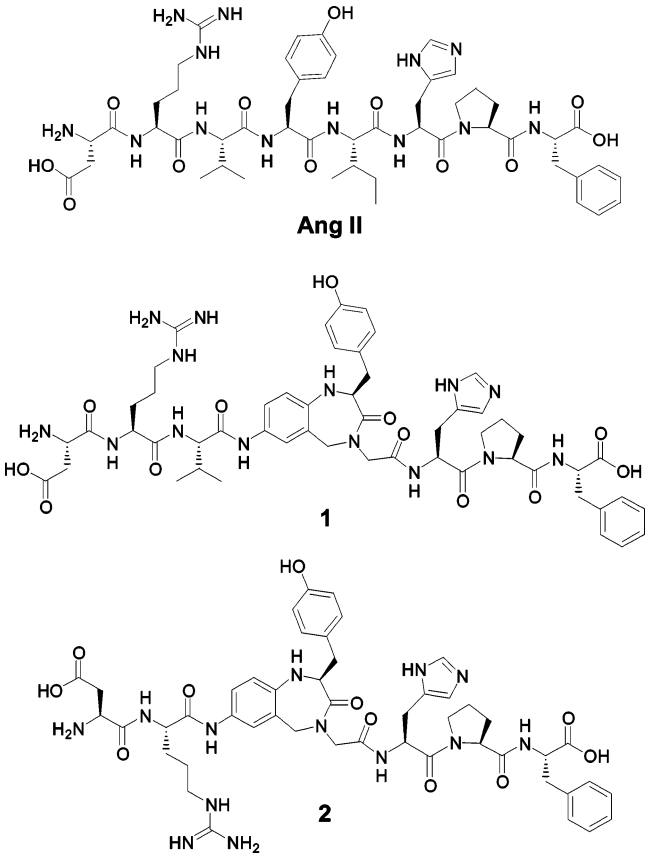

receptor affinity,[49−56] although it is known that mono- and bicyclizations in the 3−5 region of Ang II may give analogues with retained affinity.[27,29,57]

Recently, we described the Ang II derivatives (**1** and **2**) as both possessing a benzodiazepine scaffold intended to mimic a γ-turn backbone replacing either the amino acid residues 4−5 or 3−4−5 in the target peptide.[58] None of these compounds bound to the AT_1 receptor. However, compound **1**, but not compound **2**, the latter lacking the Val^3 residue, exhibited a high AT_2 receptor affinity (K_i = 3.0 nM), Chart 1. It was concluded that the position of the guanidino group of the Arg^2 residue in space, in relation to the Tyr side chain and the N-terminal end, was critical for AT_2 receptor affinity.

Molecular modeling suggested that a more favorable positioning of the Arg^2-Tyr^4 side chains could be obtained with a benzodiazepine γ-turn mimicking scaffold, where the 9-position rather than the 7-position of the benzodiazepine serves as a handle for attachment of the N-terminal residues. We herein report the design, synthesis, and binding data of the pseudopeptides **3**−**8**, comprising a new γ-turn mimic replacing the Val^3-Tyr^4-Ile^5 and Tyr^4-Ile^5 segments of Ang II (Chart 2). These compounds act as high-affinity AT_2 receptor ligands but do not bind to the AT_1 receptor. We also report that **1**, **3**, and **4** are full agonists and thus induce cell outgrowth of neurite cells, an effect that was suppressed by the selective AT_2 receptor antagonist PD123,319. Furthermore, compound **1** suppresses proliferation of PC12 cells expressing only AT_2 receptors. This is to the best of our knowledge the first report on AT_2 receptor stimulation mediated by constrained Ang II analogues.

Results

Chemistry. Two Fmoc-protected benzodiazepine-based γ-turn mimics **18a** and **18b** were synthesized in solution and thereafter incorporated into Ang II using solid-phase peptide synthesis (SPPS) to deliver the pseudopeptides **3**−**8**. The benzodiazepine core structure was used as a turn template to replace $Val^3Tyr^4Ile^5$ (**4**, **6**, and **8**) or Tyr^4Ile^5 (**3**, **5**, and **7**) in Ang II. The pseudopeptides **7** and **8** comprise the isoleucine side chain that previously has been proposed to be important for stabilizing a turn conformation at Tyr^4 in Ang II.[25,59] The synthetic routes to the γ-turn mimetics **18a** and **18b** are outlined in Scheme 1 and start with a reduction of 2-chloro-3-nitrobenzoic acid to the alcohol followed by a Swern oxidation to afford aldehyde **11** in 91% yield. The aldehyde was reacted with either the glycine equivalent 2-aminoethanol or the isoleucine equivalent (*S*,*S*)-2-amino-3-methyl-1-pentanol in reductive amination. An amino acid or its methyl ester was not employed as a building block because of the tentative formation of a diketopiperazine in a later step. Protection of the alcohol group of **12a** with *tert*-butyldiphenylchlorosilane (TBDPSCl) was performed to improve the yield and to achieve cleaner reactions. A much lower yield (20% compared to 64% over two steps) was obtained when the TBDPS-protected 2-aminoethanol was used in the reductive amination. The isoleucine derivative **12b** could be protected using the same conditions but the subsequent reaction with the TBDPS-protected alcohol **13b**, that is, the amide formation, was very slow and provided a mixture of two diastereoisomers in a low yield. Therefore, the TBDPS-protected glycine derivative **13a** and the unprotected **12b** were used in the amide coupling with Fmoc-L-Tyr(*t*-Bu)-OH using *O*-(7-azabenzothiazol-1-yl)-*N*,*N*,*N*′,*N*′-tetramethyluronium hexafluorophosphate (HATU) as the activating reagent. To further improve the yield and to considerably shorten the reaction time in the coupling of the sterically hindered **12b** with Fmoc-L-Tyr(*t*-Bu)-OH, the reaction mixture was heated to 100 °C for 15 min using controlled microwave irradiation. When these conditions are used, the Fmoc-protected product was obtained in 56% yield and only one diastereoisomer was observed in NMR. The less sterically hindered amine **13a** was reacted at room temperature overnight, and the amide was obtained in excellent yield.

Deprotection of the Fmoc group was performed using 1,8-diazabicyclo[5.4.0]undec-7-ene (DBU). Intramolecular nucleophilic aromatic substitution at the chlorine ipso carbon in **14a** proceeded smoothly in DMSO/Et_3N at 100 °C. Reacting **14b** using the same conditions gave a ∼7:3 mixture of two diastereoisomers. The diastereoisomers were separated using column chromatography, and the structural assignment and the determination of the stereochemistry of the molecules were performed using correlation spectroscopy, heteronuclear correlation spectroscopy, and rotating-frame Overhauser enhancement spectroscopy NMR experiments. The nuclear Overhauser effect (NOE) information of the intermediate **16b** and its isomer **16c** are illustrated in Figure 1. The major product in the cyclization step (**16b**) was confirmed to have *S* configuration in the ring, which is the stereochemistry of the natural amino acid used as the starting material. The minor diastereoisomer **16c**

Chart 2

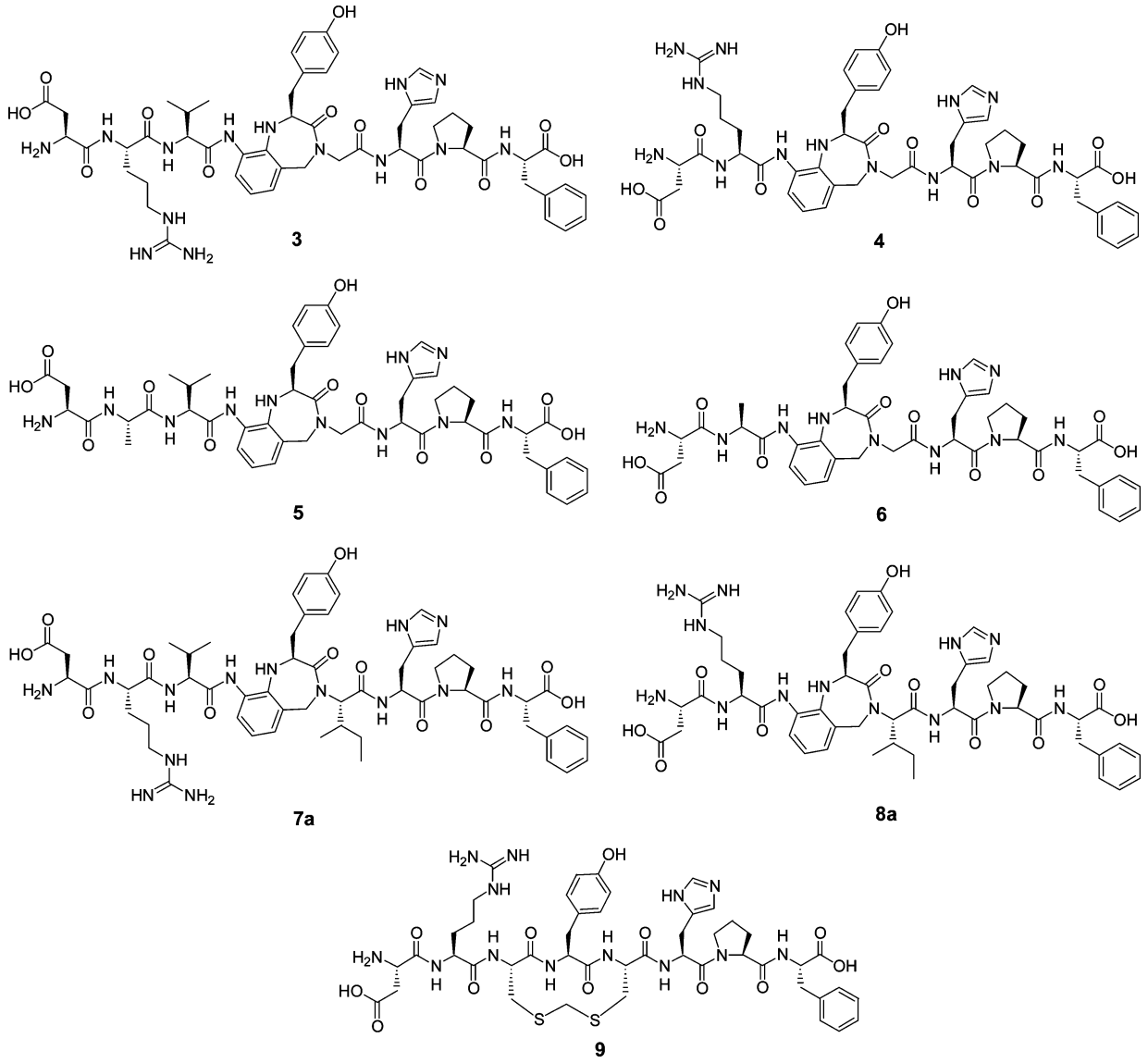

seems to have the stereochemistry outlined in Figure 1. The TBDPS-protecting group was removed from the glycine derivative **15a** using tetrabutylammonium fluoride (TBAF) in THF, and the alcohol **16a** was obtained in a good yield. Oxidation of the alcohols **16a** and **16b** was performed in two steps, first a Swern oxidation to the aldehyde and thereafter a mild oxidation using sodium chlorite at 0 °C[60] to deliver the carboxylic acids **17a** and **17b** in 90% and 76% yield, respectively. The aldehydes were not stable and were purified by extractions but could not be stored. Reduction of the nitro groups in **17a** and **17b** was performed using ammonium formate and Pd/C. The zwitterions obtained were isolated by extractions and thereafter reacted with FmocCl in dioxane and aqueous Na_2CO_3. The pure compound **18a** was obtained in 68% yield using repeated extraction while the reduction and/or protection of **17b** produced an ~8:2 mixture of diastereoisomers. After purification by reversed-phase high-performance liquid chromatography (RP-HPLC), the major component **18b** was obtained in 35% yield.

Incorporation of the Fmoc derivatives **18a** and **18b** into Ang II using standard Fmoc/*t*-Bu SPPS methodology produced the pseudopeptides **3**−**6** and **7**−**8**, respectively. The protected γ-turn mimetics **18a** or **18b** were manually coupled to the His(Trt)-Pro-Phe-Wang-resin in DMF using PyBOP as an activating agent and diisopropylethylamine (DIEA) as a base. Prolonged reaction times were used for the incorporation of the turn templates and the adjacent amino acids where the couplings were expected to proceed slowly. After completion of the synthesis, TFA in the presence of water and triethylsilane was used to liberate the target peptides from the resin. The products were precipitated with diethyl ether and purified by RP-HPLC. Compound **18a** gave the single pseudopeptides **3**−**6**, while compound **18b** produced two diastereoisomers of the pseudopeptides **7** and **8** in ~5:1 and ~2:1 ratios, respectively. The diastereoisomers could be separated in the final purification step to give **7a**, **7b**, **8a**, and **8b** (**a** and **b** denote single diastereoisomers of unassigned absolute stereochemistry). When the intermediate **16b** corresponded to the natural L-configuration, we hypothesize that the stereochemistry of the major products (**7a** and **8a**) also corresponds to the natural L-configuration.

Binding Assays. Radioligand binding assays relying on the displacement of [^{125}I]Ang II from AT_1 receptors in rat liver membranes[61] and from AT_2 receptors in pig

Scheme 1[a]

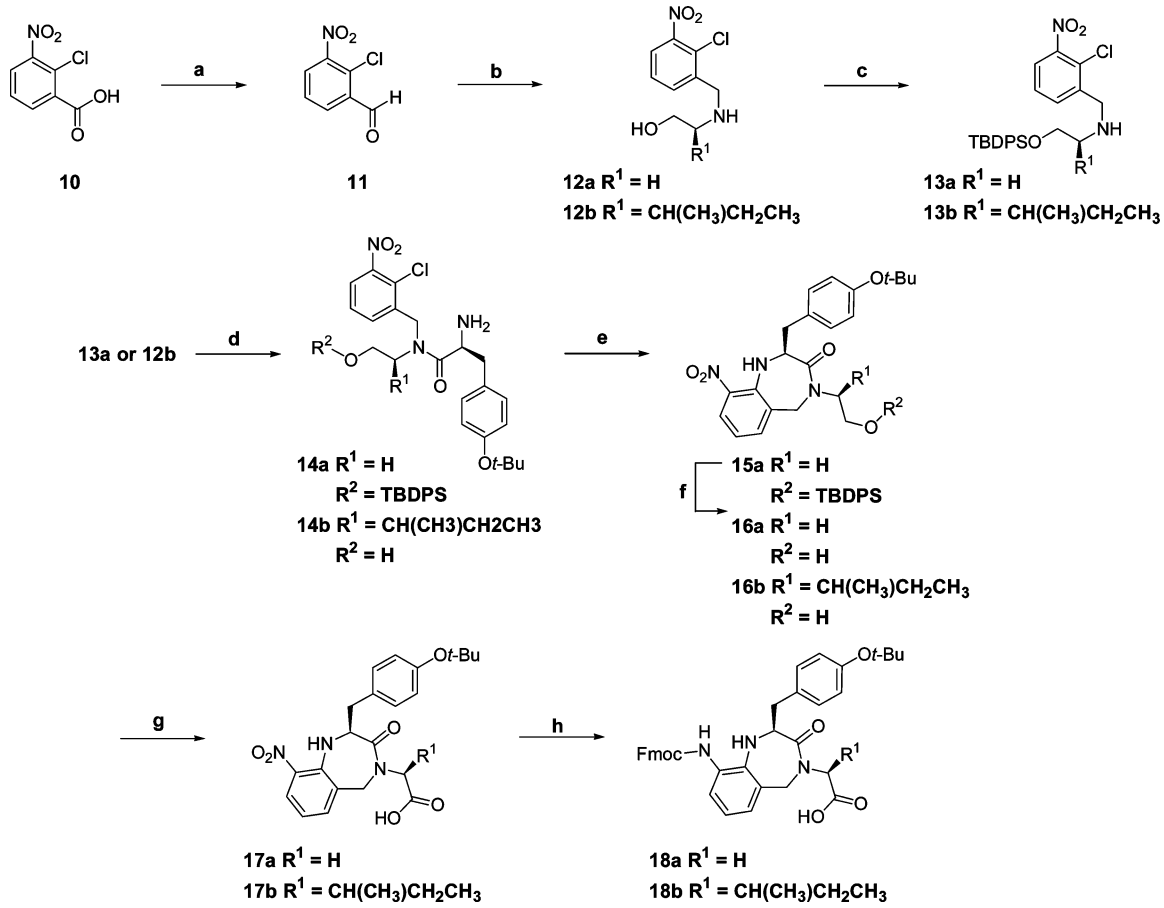

[a] Reagents: (a) (i) $NaBH_4$, $BF_3{\cdot}Et_2O$, THF, (ii) ClCOCOCl, DMSO, Et_3N, CH_2Cl_2, 91%; (b) 2-aminoethanol or (*S*,*S*)-2-amino-3-methyl-1-pentanol, HOAc, $NaCNBH_3$, MeOH, 56−69%; (c) *tert*-butylchlorodiphenylsilane, DBU, THF, 85−93%; (d) (i) Fmoc-L-Tyr(*t*-Bu)-OH, HATU, DIEA, CH_2Cl_2, (ii) DBU, THF, 46−90%; (e) Et_3N, DMSO, 41−82%; (f) TBAF, THF, 89%; (g) (i) oxalyl chloride, DMSO, Et_3N, CH_2Cl_2, (ii) $NaClO_2$, NaH_2PO_4, cyclohexene, *t*-BuOH, H_2O, 76−86%; (h) (i) $HCOONH_4$, Pd/C, MeOH, (ii) FmocCl, Na_2CO_3 (aq), dioxane, 35−68%.

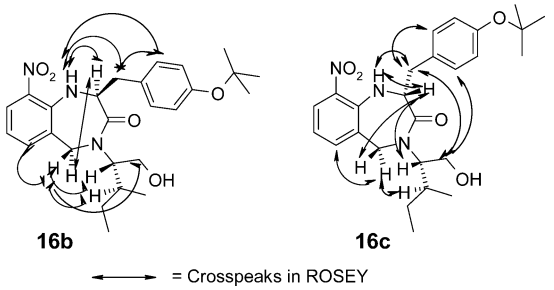

Figure 1. NOE information from the major diastereoisomer **16b** and the minor diastereoisomer **16c**.

uterus membranes[62] were used to evaluate compounds **3**−**8** (Table 1). The natural ligand Ang II and the AT_2 receptor selective agonist [4-NH_2-Phe^6]Ang II[53] were used as reference substances. Compound **1** has previously been reported to have a high affinity to the AT_2 receptor (K_i = 3.0 nM) while compound **2**, without the extra Val residue, lacks affinity to the AT_2 receptor (K_i > 10 μM).[58] In contrast, the pseudopeptides **3** and **4** encompassing the new γ-turn mimetic **18a**, exhibit both good binding affinity and high AT_2/AT_1 receptor selectivity (Table 1). Compound **3**, incorporating a Val residue, has a slightly better binding affinity (K_i = 0.8 nM) than compound **4** (K_i = 2.8 nM). Replacement of the Arg^2 residue in compounds **3** and **4** with Ala gave compounds **5** and **6**, respectively. In both of these compounds the binding affinity was reduced by a factor of 10. The pseudopeptides **7a** and **8a** encompassing the γ-turn mimetic **18b**, with an isoleucine side chain in the $i + 2$ position, both have good binding affinity for the AT_2 receptor. Compound **7a**, with a Val residue, exhibits a K_i of 0.3 nM and **8a**, without the Val residue, a K_i of 2.6 nM. Interestingly, **7b**, the diastereoisomer of **7a**, exhibits an even better binding affinity for the AT_2 receptor (K_i = 0.08 nM) while **8b**, the diastereoisomer of **8a**, has a moderate binding affinity (K_i = 117.4 nM). None of the pseudopeptides displayed any affinity for the AT_1 receptor. Compounds **1**, **3,** and **4**, with defined stereochemistry, were chosen for further more advanced in vitro studies.

Table 1. Binding Affinities for the AT_1 and AT_2 Receptors

compound	AT_1 (rat liver membranes) K_i (nM) ± SEM	AT_2 (pig uterus myometrium) K_i (nM) ± SEM
Ang II	0.24 ± 0.07	0.23 ± 0.03
[4-NH_2-Phe^6]Ang II	>10000	0.9 ± 0.3
1	>10000[58]	3.0 ± 1.1[58]
2	>10000[58]	>10000[58]
3	>10000	0.8 ± 0.1
4	>10000	2.8 ± 0.2
5	>10000	9.3 ± 1.4
6	>10000	37.4 ± 2.1
7a	>10000	0.3 ± 0.01
7b	>10000	0.08 ± 0.003
8a	>10000	2.6 ± 0.2
8b	>10000	117.4 ± 7.7

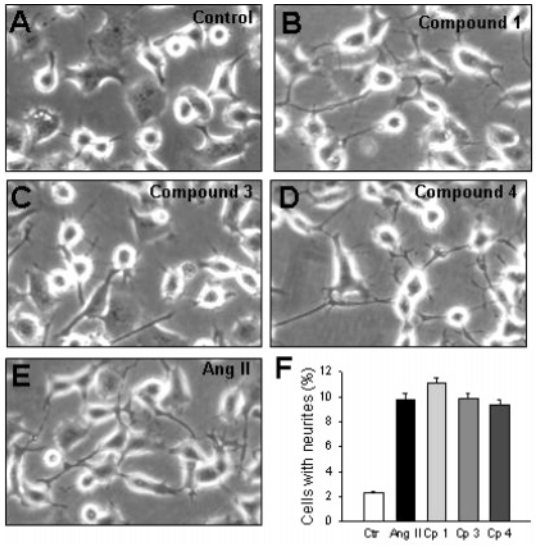

Figure 2. Comparative effects of the three compounds **1**, **3,** and **4** and angiotensin II (Ang II) on neurite outgrowth in NG108-15 cells. NG108-15 cells were plated at a density of 4 $\times$ 10^4 cells per dish in 35 mm Petri dishes and were cultured for 3 days in the absence (control (A)), or in the presence of 0.1 μM **1** (B), 0.1 μM **3** (C), 0.1 μM **4** (D), or 0.1 μM Ang II (E). Neurite outgrowth was quantified as explained in the Experimental Section (F). All panels are seen at the same magnification.

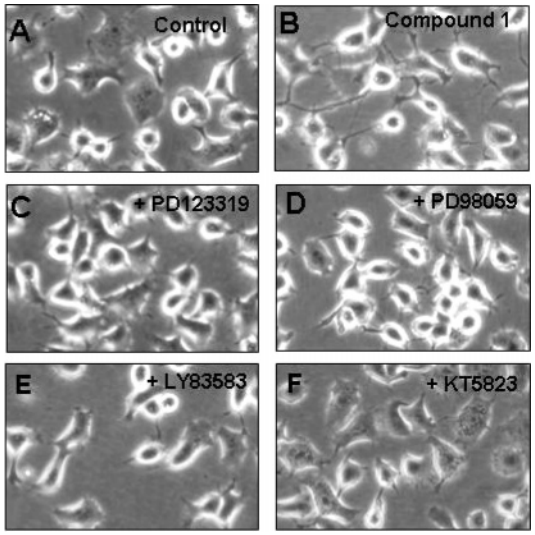

Figure 3. Various inhibitors effect on neurite outgrowth in NG108-15 cells induced by compound **1**. NG108-15 cells were plated at a density of 4 $\times$ 10^4 cells per dish in 35 mm Petri dishes and were cultured for 3 days in the absence (control (A)) or in the presence of 0.1 μM **1** (B) or in the presence of compound **1** (0.1 μM) and 1 μM PD123,319 (C), compound **1** (0.1 μM) and 10 μM PD98,059 (D), compound **1** (0.1 μM) and 0.5 μM LY-83,583 (E), or compound **1** (0.1 μM) and 1 μM KT 5823 (F). All panels are seen at the same magnification.

In Vitro Morphological Effects Induced by Compounds 1, 3, and 4 in NG 108-15 Cells. To study the effects of compounds **1**, **3**, and **4** on differentiation, NG108-15 cells were used. In their undifferentiated state, neuroblastoma $\times$ glioma hybrid NG108-15 cells have a rounded shape and divide actively. We have shown previously that these cells express only the AT_2 receptor[63,64] and that a 3 day treatment with Ang II or the selective peptidic AT_2 receptor agonist CGP 42112 induces neurite outgrowth.[64] The mechanisms involve a sustained increase in p42/p44^{mapk} activity[23,24] and activation of the nitric oxide/guanylyl cyclase/cGMP pathway[65] (for review see ref 8).

For all experimental conditions, cells were plated at the same initial density (4 $\times$ 10^4 cells/35 mm Petri dish) and were treated with Ang II or one of the pseudopeptides **1**, **3**, or **4**. After 3 days of culture, the cells were examined under a phase-contrast microscope and micrographs were taken. The pseudopeptides were first tested at various concentrations ranging from 1 pM to 1 μM. Except for the higher concentration of 1 μM, none of the other doses induced cell death. In addition, in cells stimulated for 3 days with concentrations higher than 0.1 nM, the three tested pseudopeptides induced neurite outgrowth. As shown by phase-contrast microscopy, nontreated control cells had rounded cell bodies, without or with some thin processes (Figure 2A). After a 3 day treatment with **1** (Figure 2B), **3** (Figure 2C), or **4** (Figure 2D) (0.1 μM), most cells extended one or two neurite processes exhibiting a growth cone at the tip,[64] while the cell body retained a rounded appearance. In comparison to Ang II (0.1 μM) (Figure 2E), the tested compounds induced the same morphological changes.[64] Quantification of these results indicated that a 3 day treatment with **1**, **3**, or **4** increased the number of cells with neurites longer than one cell body from 2.26 $\pm$ 0.10% in control cells to 11.07 $\pm$ 0.46%, 9.88 $\pm$ 0.41%, and 9.35 $\pm$ 0.35% in the cells treated with compounds **1**, **3**, and **4**, respectively (Figure 2F). This effect was mediated through the AT_2 receptor, since coincubation of **1**, **3**, or **4** with the AT_2 receptor antagonist, PD123,319 (1 μM), virtually halted neurite elongation. An illustration is shown in Figure 3C for compound **1**. Similar observations were made with compounds **3** and **4**. We have previously shown that PD123,319 alone did not alter the morphology of the untreated cells.[23,64]

To further explore if compounds **1**, **3**, and **4** share the same signaling transduction as Ang II,[23,65] cells were preincubated for 3 days with 10 μM PD98,059: a dose that abolished MAPK activity. When coincubated with **1**, **3**, or **4**, PD98,059 decreased the length and number of neurites (Figure 3D). Cells were also preincubated with LY-83,583 (0.5 μM), an inhibitor of soluble guanylyl cyclase (sGC) or with KT 5823 (1 μM), an inhibitor of cGMP-dependent protein kinases. PD98,089, LY-83,583, and KT 5823 treated cells had the same morphological appearance alone as the control, untreated cells. However, cells coincubated with **1**, **3**, or **4** and LY-83,583 or KT 5823 have only one or two thin processes (parts E and F of Figure 3). Treatment with Ang II increased the number of cells by 9.74 $\pm$ 0.51%. This effect was abolished in cells coincubated with PD123,319, PD98,-059, LY-83,583, and KT 5823 (Figure 4).

The pseudopeptides **1**, **3**, and **4** also induced phosphorylation of p42/p44^{mapk}, as determined by using an antibody directed against the phosphorylated form of p42/p44^{mapk}. Thirty minutes of application (optimum time period for maximal effect of Ang II)[23,65] of compound **1**, **3**, or **4** stimulated phosphorylation of p42/p44^{mapk} with a (2.2 $\pm$ 0.2)-, (2.8 $\pm$ 0.9)-, and (2.9 $\pm$ 0.4)-fold increase over control, respectively. The stimulation was abolished in cells preincubated with 10 μM PD123,-319 or 10 μM PD98,059 (Figure 5).

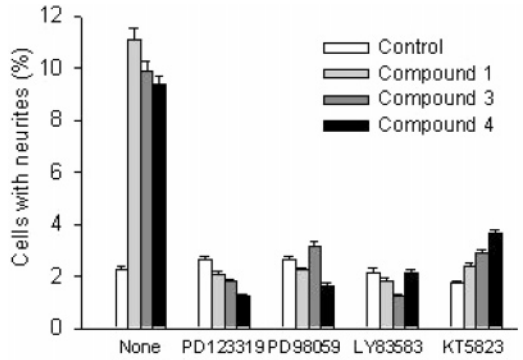

Figure 4. Various inhibitors effects on neurite outgrowth in NG108-15 cells induced by compounds **1**, **3**, and **4**. Cells with at least one neurite longer than a cell body were counted as positive for neurite outgrowth The number of cells with neurites represent the percentage of the total number of cells in the micrographs (from 50 to 100 cells according to the experiment). The control bar in each experiment corresponds to an experiment with only the reference compound.

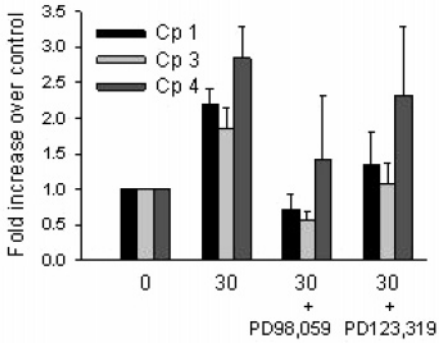

Figure 5. The effect of compounds **1**, **3**, and **4** on p42/p44^{mapk} activation. NG108-15 cells were stimulated without or with 0.1 μM of the Ang II analogues **1**, **3**, or **4** for 30 min alone or in the presence of 10 μM PD123,319 or 10 μM PD98,059.

Table 2. Proliferation of PC12 Cells as Measured with [^{3}H]thymidine Incorporation

	counts per minute
10% FCS	62585 ± 3853
10% FCS + 1.0 μM Ang II	48887 ± 3737[a]
10% FCS + 1.0 μM PD123,319	68707 ± 3483
10% FCS + 1.0 μM compound **1**	45421 ± 2883[a]

[a] $p < 0.05$ vs 10% FCS only, $n = 10-12$.

Proliferation of PC12 Cells. It was also investigated whether compound **1** could inhibit proliferation of PC12 cells only expressing AT_2 receptors.[66] As shown in Table 2, compound **1** inhibited proliferation of cells grown in 10% FCS to the same extent as Ang II at 1.0 μM.

Molecular Modeling. A conformational analysis was performed on **20** and **21**, Figure 6, but with Ala replacing Tyr, which resulted in 10 and 11 conformations, respectively, within 5 kcal/mol of the lowest energy minimum. The lowest energy conformations were used in the geometrical comparison shown in Figure 7. The distances and angles in the other conformations of each structure were within 0.1 Å and 5°, respectively. A minimized peptide structure of an ideal inverse γ-turn was also included for comparison.

Scaffold **21** was further studied to see if a corresponding peptide γ-turn could be identified in a crystallized protein. The conformations within 1 kcal/mol of the

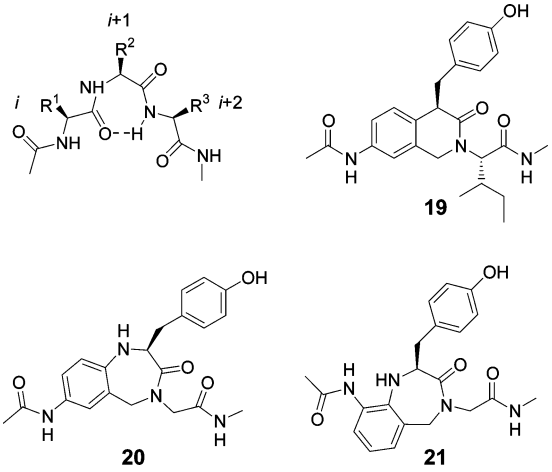

Figure 6. A γ-turn with the i, $i + 1$, and $i + 2$ residues indicated and scaffolds that have been used as γ-turn mimetics.

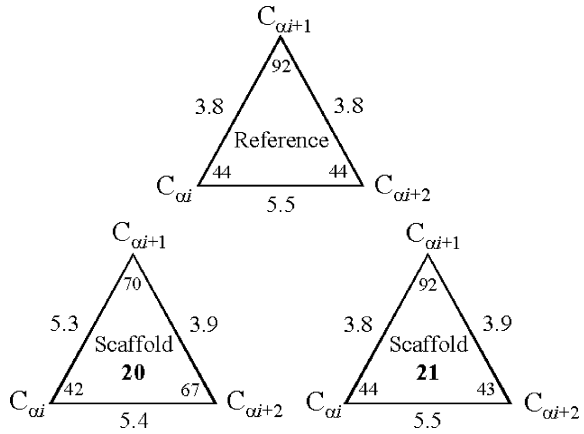

Figure 7. A comparison of scaffolds **20** and **21** with respect to distances and angles between the C_α atoms. The measured distances are given outside, and the angles inside, the triangle. The aromatic carbon connected to the N-terminal handle is selected as $C_{\alpha i}$. The top triangle shows distances and angles in a minimized ideal inverse γ-turn.

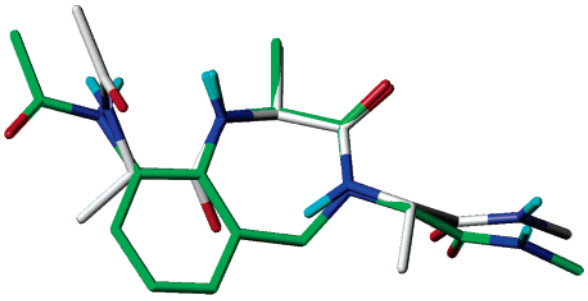

Figure 8. The γ-turn mimetic **21** (green) and a γ-turn from a crystallized protein (gray) superimposed.

lowest energy minimum (three conformations) were evaluated by comparing the torsion angles Φ_i, Ψ_i, Φ_{i+1}, Ψ_{i+1}, Φ_{i+2}, and Ψ_{i+2} in **21** with the corresponding torsion angles in γ-turns from an in-house database of 2101 extracted inverse γ-turns from protein X-ray structures from the protein data bank (PDB).[67] The third lowest energy conformation compared well to an inverse γ-turn in the database (PDB ID: 1NNF, chain A, sequence Thr^{82}-Ala^{83}-Gln^{84}). A superimposition of these structures can be seen in Figure 8.

Using the pharmacophore modeling program DISCOtech[68], we investigated if the active compounds **1**, **3**,

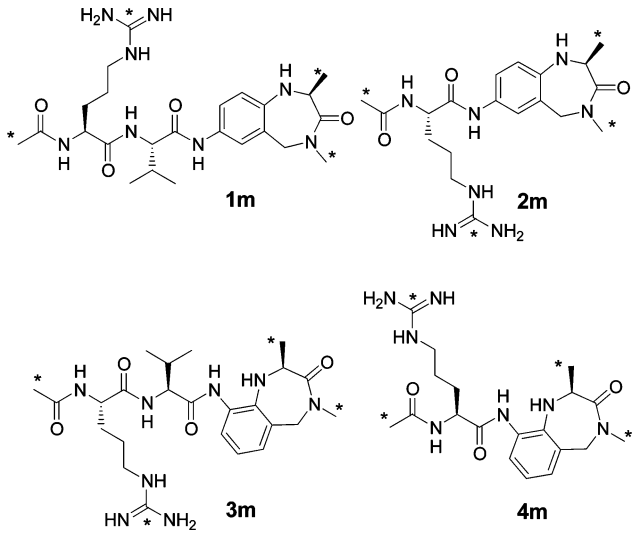

Figure 9. Model compounds used in the conformational analysis and molecular modeling. Asterisks indicate atoms used for comparison between conformations in the conformational analysis. These atoms also correspond to the DISCOtech features (the guanidino carbon only indirectly).

and **4** could position important structural elements (features) in common regions of space not accessible to the inactive compound **2**. In this study model compounds **1m**, **2m**, **3m**, and **4m** were used, and the structural elements included were, see Figure 9, (a) the Ala side chain (corresponding to C_β in the Tyr residue in the full-length pseudopeptides), (b) the C-terminal benzodiazepine anchor point (corresponding to C_α in Gly), (c) the binding site in the receptor corresponding to the Arg guanidino group (as defined by DISCOtech), and (d) the N-terminal end (corresponding to C_α in Asp). DISCOtech requires as input a set of conformations (max 300) of each compound. These were generated with a Monte Carlo search in MacroModel 8.5[69] using the MMFFs force field and the generalized Born solvent accessible surface area (GB/SA)[70] water solvation model. To reduce the number of conformations and to identify a representative set of conformations (<300) for each compound, we removed those where the guanidino group participates in an intramolecular hydrogen bond to a carbonyl oxygen. In our hypothesis of the receptor-bound conformation of Ang II, the Arg side chain is interacting with Asp^{297} (see refs 71 and 72) and should therefore not be intramolecularly hydrogen bonded. The number of conformations found within 5 kcal/mol of the energy minimum for **1m**, **3m**, and **4m** (Figure 9) were 3704, 620, and 3207, respectively. By removing very similar conformations, we were able to reduce the number of conformations further. This was accomplished by minimization with (a) increased convergence criterion, (b) a reduced number of atoms for identifying unique conformations (only the atoms that represent a feature in the later DISCOtech run), and (c) the distance between atoms compared for defining unique conformations (BatchMin CRMS command) set to 0.75 Å for **3m** and to 1.5 Å for **1m** and **4m** (the 1.5 Å value for **1m** and **4m** was used to arrive at less than 300 conformations). The number of conformations found with this protocol for **1m**, **3m**, and **4m** was 212, 167, and 158, respectively. DISCOtech identified 82 different models with superimposed conformations where the important

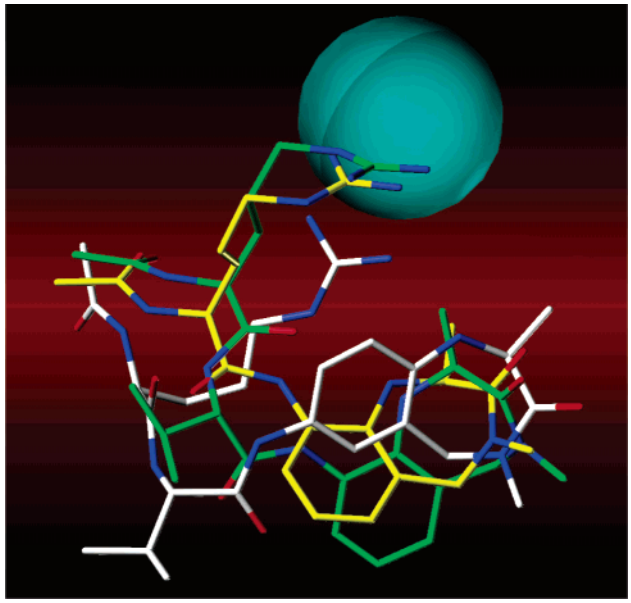

Figure 10. The model of superimposed structures obtained by DISCOtech that has the highest structural overlap. **1m** is shown with white carbons, **3m** with green carbons, and **4m** with yellow carbons. The cyan sphere indicates the hydrogen bonding acceptor site in the receptor.

elements were positioned in the same space. However, many of the models had very low overall structural overlap and were therefore not convincing. To select the most relevant model(s), the total van der Waals volume of each model was calculated. A small total volume indicates a high structural overlap, and a large total volume, when the structures are not matched, indicates a low structural overlap. The model with the lowest total volume is shown in Figure 10. This model corresponds to a plausible binding mode for the active compounds with each of the four investigated structural elements confined within 2.5 Å for all three structures.

An additional DISCOtech analysis including **2m** was performed to investigate if the inactive compound could fit this model as well. With the same protocol as above (with CRMS set to 0.75 Å), the number of conformations identified for **2m** was initially 687 and after refinement 237. The same DISCOtech protocol was applied, and 57 models were found. However, none of these models had a convincing alignment, and none of the conformations included in the previous model (Figure 10) were present in any of these new models. This indicates that the active compounds may have a common binding mode not accessible to the inactive compound.

Discussion

Until recently only a small set of receptor selective compounds have been available for the functional studies of the AT_2 receptor, for example, PD123,319,[73] CGP-42112,[74] and (4-NH_2-Phe^6)Ang II,[53] the latter being used as a reference compound in the present study. We recently disclosed the first selective nonpeptidic AT_2 receptor agonist,[75] developed from a nonselective AT_1/AT_2 receptor agonist[76−78] structurally related to the "sartans". However, our major research interest and long-term objective is to enable transformation of peptides to druglike non-peptides via incorporation of well-defined mimetics of secondary structure motifs in the

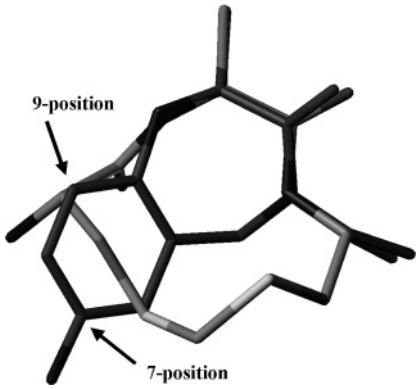

Figure 11. Superimposition of the γ-turn moieties of **9** and **20**. The 7- and 9-position in the benzodiazepine skeleton are indicated by arrows.

target peptides. For example, several cyclic analogues of Ang II have been synthesized and assessed as ligands to the AT_2 receptor.[27,29] One of the most potent ligands (K_i = 0.62 nM), a monocyclic methylenedithioether analogue of Ang II (**9**), was found to preferentially adopt low-energy inverse γ-turn conformations centered at Tyr^4, as deduced from the conformational analysis.[27] We reasoned that incorporation of suitable rigid scaffolds mimicking this inverse γ-turn should constitute a relevant first approach in the search for the bioactive conformation(s) of Ang II when binding and activating the AT_2 receptor.

The isoquinoline **19** and the benzodiazepine **20** have previously been employed as scaffolds mimicking the presumed γ-turn centered at Tyr^4 in Ang II (Figure 6).[45,58] Substitution of Val^3-Tyr^4-Ile^5 of Ang II by the isoquinoline **19** renders an AT_2 receptor ligand with a K_i of 61 nM, while the same substitution with the benzodiazepine **20** provides an inactive pseudopeptide (**2**).[58] When a Val^3 residue was introduced in **2** and only the Tyr-Ile peptide segment was substituted, a highly potent analogue (**1**) was obtained with a K_i of 3 nM.[58] Using **9** as a reference peptide, we hypothesized that the reason for the lack of affinity of the shorter peptide **2** was not that the Val^3 was missing per se but rather that the guanidino group of the Arg^2 residue and/or the N-terminal part of the pseudopeptide could not interact optimally with the receptor due to the geometric difference between **2** and **9**. The main reason for this is that the γ-turn moiety in **1** and **2** is not optimal from a geometrical point of view (Figure 7). However in peptide **1**, Val^3 could function as a spacer and allow the Arg residues and the N-terminal part in **1** and **9** to interact in similar positions despite the geometric difference.

When the γ-turn moieties of **20** and **9** are superimposed (Figure 11), it can be seen that by moving the entry point of the peptide chain in the benzodiazepine scaffold from the 7-position to the 9-position a geometrically better γ-turn mimetic could be obtained (**21** in Figure 6). This is shown in more detail in Figure 7 where a γ-turn in a reference peptide and the γ-turn mimetics **20** and **21** and some key distances and angles are compared. In this comparison, we used the inverse γ-turn conformation of the peptide and focused on the distances and angles between the three C_α atoms within the γ-turn moiety. It can be seen that the reference γ-turn and the mimetic **21** are very similar. We also compared the benzodiazepine scaffold with peptide backbones as illustrated in Figure 8, where **21** is compared to a γ-turn found in a crystallized protein. Taken together, this shows that scaffold **21** resembles more the native γ-turn than **20**. When **21** is used as a γ-turn mimetic, it could also allow the pseudopeptide without the extra Val residue to reach the common regions of space and possibly pick up affinity. This prompted us to synthesize both compound **3** with the extra Val residue, and compound **4** and evaluate the AT_2 receptor binding affinities.

Both pseudopeptides **3** (K_i = 0.8 nM) and **4** (K_i = 2.8 nM) exhibited high affinity to AT_2 receptors. It seems that the extra valine residue is not required for optimal interaction with the receptor when scaffold **21** is used, which supports our hypothesis. When the arginine residue in pseudopeptide **1** was replaced with an alanine, all of the AT_2 receptor affinity was lost.[58] Interestingly, when the same substitution was made in pseudopeptides **3** and **4**, the affinity for the obtained compounds, **5** and **6**, only dropped 10 times. This is more in line with the decrease in affinity that is observed when $arginine^2$ is substituted by glycine[56] or glutamine[49] in Ang II. It therefore seems that **3**, **4**, and Ang II interact similarly with the AT_2 receptor. The reason for the large decrease in affinity for **1** is most likely because of the removal of the Arg side chain in combination with a nonoptimal interaction with the receptor.

To study if compounds **1**, **3**, and **4**, which all have high affinity to the AT_2 receptor, could adopt similar conformations, we superimposed key features in the molecules using the pharmacophore search program DISCOtech. Among the identified models, one held all the included groups in the same areas and had a reasonable scaffold alignment (see Figure 10). This shows that although the three active molecules encompass quite different scaffolds, they can still adopt the same binding mode/interaction pattern. This model had no equivalent among the models found when the inactive molecule (**2**) was included in the analysis.

Another interesting observation that can be made from the analysis is that the valine side chains of **1** and **3** are located in the same region in the model (see Figure 10). This could imply that the valine not only allowed for a better receptor alignment due to the extra flexibility but also may be of some importance for direct receptor interaction. This interaction may be the reason for the moderate increase in affinity when the extra valine is inserted in **4** to give **3**, since a reasonable receptor alignment already seems to have been obtained for both of these compounds.

The lipophilic side chains Val^3 and Ile^5 in Ang II are considered to have only conformational stabilizing roles and to induce a turn motif when Ang II interacts with the AT_1 receptor.[25,59] It has also been indicated that these side chains are less important for Ang II binding to the AT_2 receptor.[49,56] Therefore, to study the impact of the lipophilic side chain Ile^5 for affinity in the pseudopeptide **3,** we synthesized and evaluated compounds **7a** and **8a** (Chart 2). Compound **7a** had approximately the same binding affinity to the AT_2 receptor as the analogue without the Ile side chain (**3**) K_i = 0.3 nM and K_i = 0.8 nM, respectively. The two analogues that did not contain the extra valine residue (**4** and **8a**) also had very similar binding affinities to

the AT_2 receptor. Compound **8a** exhibited a K_i of 2.6 nM compared to a K_i of 2.8 nM for pseudopeptide **4** without the Ile side chain. These results indicate that the Ile side chain can be omitted in the turn templates without affecting the binding affinities. While compounds **7a** and **8a** were synthesized, partial epimerization took place, and two additional compounds (**7b** and **8b**) could be isolated and evaluated. Interestingly, pseudopeptide **7b**, a diastereoisomer to compound **7a** exhibited a very good binding affinity to the AT_2 receptor ($K_i = 0.08$ nM). In contrast, the diastereoisomer of compound **8a**, pseudopeptide **8b**, had only a moderate binding affinity ($K_i = 117.4$ nM) to the AT_2 receptor. Notably, the absolute stereochemistry of neither **7b** nor **8b** has been determined. All the synthesized pseudopeptides lacked affinity ($K_i > 10\,000$ nM) to the AT_1 receptor.

To establish if these compounds are agonists or antagonists, we selected compounds **1**, **3**, and **4** and evaluated their potential for inducing neurite outgrowth and antiproliferation. The present results demonstrate that the three tested pseudopeptides (**1**, **3**, and **4**) induce neurite outgrowth, one of the first steps of neuronal differentiation, as does Ang II and CGP-42112.[64] In addition, **1**, **3**, and **4** as well as Ang II stimulate MAPK activity, and as previously shown,[23] this activation of the p42/p44^{mapk} pathway is essential to promote neurite outgrowth by cells stimulated with **1**, **3,** or **4**. These effects are attributabed to the AT_2 receptor, since coincubation with PD123,319 abolishes the effect. Moreover, inhibition of cGMP-dependent kinases with KT 5823 or sGC with LY-83,583 indicate that cGMP participates in the early steps of neurite elongation suggesting that compounds **1**, **3,** and **4** induce neurite outgrowth through MEK/p42/p44^{mapk} and the nitric oxide/guanylyl cyclase/cGMP pathway. All of these results corroborate previous observations made with Ang II or the peptide agonist CGP-42112,[23,64,65] indicating that the pseudopeptides **1**, **3**, and **4** act as agonists at the AT_2 receptor. Compound **1** also inhibits proliferation of PC12 cells only expressing AT_2 receptors, a finding which further supports the view that pseudopeptide **1** acts as an agonist.

The nonpeptidic AT_2 selective agonist that we previously reported[75] lacks structural elements that are likely to mimic the N-terminal (Asp-Arg-Val-Tyr-Ile) of Ang II, but the compound is still serving as a full AT_2 receptor agonist. Thus, Ang II and the pseudopeptide agonists **1**, **3**, and **4** reported herein and the nonpeptidic agonist seem to bind very differently to the AT_2 receptor, which is essentially in accordance with the similar findings by Perlman et al. regarding AT_1 receptor activation.[77]

Conclusion

A new, improved γ-turn mimetic with one or two amino acid side chains has been synthesized and incorporated into Ang II. The resulting pseudopeptides showed high AT_2 receptor affinity and selectivity. The three compounds selected for agonist evaluation were shown to induce neurite outgrowth and stimulate p42/p44^{mapk}, and furthermore, one was shown to suppress proliferation of PC12 cells. It can therefore be concluded that these pseudopeptides act as agonists at the AT_2 receptor. Furthermore, it has been demonstrated by molecular modeling that, for the bioactive compounds, key structural elements can reach common regions in space and therefore probably bind to the AT_2 receptor in a similar fashion. A successful design of organic scaffolds mimicking the secondary structure adopted by Ang II when interacting with the AT_1 receptor remains a challenge.

Experimental Section

General Methods. ^{1}H and ^{13}C NMR spectra were recorded on a JEOL JNM-EX400 at 400 and 100.5 MHz, respectively, or a Varian MERCURY+ 400 spectrometer (400 MHz). Spectra were recorded at ambient temperature unless otherwise noted. Chemical shifts are reported as δ values (ppm) referenced to δ 7.26 $CHCl_3$, δ 77.0 $CDCl_3$, δ 3.30 CH_3OH, δ 49.15 CD_3OD, δ 2.50, and δ 39.5 DMSO-d_6. Optical rotations were measured on a Perkin-Elmer model 241 polarimeter. Analytical Laboratories, Lindlar, Germany, performed the elemental analyses. Analytical reversed-phase liqiud chromatography−mass spectrometry (RP LC−MS) was performed with a Gilson HPLC system combined with a Finnigan AQA quadropole mass spectrometer using a Chromolith Performance RP-18e column at a flow rate of 4 mL/min. Preparative RP LC−MS was performed using an identical LC-MS system but with a Zorbax SB-C8, 5 μm column (21.2 mm × 150 mm) at a flow rate of 15 mL/min.

Thin-layer chromatography (TLC) was performed using aluminum sheets precoated with silica gel 60 F_{254} (0.2 mm, E. Merck). The spots were identified by UV detection and/or by spraying with a 3% methanolic solution of ninhydrin followed by heating. Flash column chromatography was performed using Merck silica gel 60 (40−63 μm). The microwave reactions were conducted in heavy-walled glass Smith process vials (5 mL) sealed with aluminum crimp caps that were fitted with a silicon septum. The microwave heating was performed in a Smith synthesizer single-mode microwave cavity (Biotage, Uppsala, Sweden).

2-Chloro-3-nitrobenzaldehyde,[79,80] **11.** 2-Chloro-3-nitrobezoic acid (10.00 g, 49.6 mmol) in THF (50 mL) was added dropwise over 50 min to an ice-cooled suspension of sodium borohydride (3.60 g, 94.7 mmol) in THF (160 mL). The solution was treated dropwise with boron trifluoride etherate (18 mL, 142 mmol) over 30 min. The reaction mixture was stirred for 5 h at room temperature, cooled on an ice bath, and acidified with 1 M hydrochloric acid. EtOAc and water were added, the layers were separated, and the aqueous layer was extracted with EtOAc. The combined organic layers were washed with water, saturated $NaHCO_3$, water, 1 M hydrochloric acid, and brine, dried ($MgSO_4$), and evaporated to give (2-chloro-3-nitrophenyl)methanol[79] (8.90 g, 96%) as a white solid. Anal. ($C_7H_6ClNO_3$) C, H, N. A solution of oxalyl chloride (2.74 mL, 32.0 mmol) in CH_2Cl_2 (140 mL) was cooled to −78 °C. DMSO (4.80 mL, 67.7 mmol) was added dropwise, and the mixture was stirred for 15 min before a solution of (2-chloro-3-nitrophenyl)methanol (4.00 g, 21.3 mmol) in CH_2Cl_2 (40 mL) was added dropwise during 20 min. The reaction mixture was stirred for 1 h at −78 °C before Et_3N (15.0 mL, 108 mmol) was added, and the reaction temperature was allowed to reach −30 °C in 40 min. Water and more CH_2Cl_2 were added, and the layers were separated. The aqueous layer was extracted with CH_2Cl_2, and the combined organic layers were washed with 1 M $KHSO_4$, water, saturated $NaHCO_3$, and brine, dried over Na_2SO_4, and evaporated. The benzaldehyde **11** was obtained as a beige solid (3.76 g, 95%). Anal. ($C_7H_4ClNO_3$) C, H, N.

2-(2-Chloro-3-nitro-benzylamino)ethanol, 12a. HOAc (0.39 mL, 6.83 mmol) and 2-aminoethanol (1.26 mL, 20.9 mmol) were added to a solution of **11** (773 mg, 4.16 mmol) in MeOH (45 mL). After 10 min, $NaCNBH_3$ (290 mg, 4.62 mmol) was added and the reaction mixture was heated to reflux for 3 h. The mixture was cooled to room temperature, acidified to pH 1 by addition of 2 M HCl, and partly evaporated. The

residue was washed with diethyl ether, and 6 M NaOH was added to adjust the pH to 11. The water layer was extracted with diethyl ether, and the combined organic layers were dried over Na_2SO_4 and evaporated to give the alcohol **12a** as a yellow solid (665 mg, 69%). Anal. ($C_9H_{11}N_2O_3$) C, H, N.

[2-(*tert*-Butyldiphenylsilanyloxy)ethyl]-(2-chloro-3-nitrobenzyl)amine, 13a. DBU (1.00 mL, 6.69 mmol) and TBDPSCl (1.70 mL, 6.64 mmol) were added to an ice-cooled solution of the alcohol **12a** (1.30 g, 5.64 mmol) in CH_3CN (30 mL). The reaction mixture was stirred for 5 h at room temperature. After evaporation the residue was dissolved in water and EtOAc and extracted with EtOAc. The combined organic layers were washed with water and brine, dried (Na_2SO_4), and evaporated. Purification by column chromatography (EtOAc/pentane, 1:4) gave **13a** as a pale yellow oil (2.46 g, 93%). Anal. ($C_{25}H_{29}ClN_2O_3Si$) C, H, N.

(2S)-2-Amino-3-(4-*tert*-butoxy-phenyl)-*N*-[2-(*tert*-butyldiphenylsilanyloxy)ethyl]-*N*-(2-chloro-3-nitrobenzyl)-propionamide, 14a. The amine **13a** (2.30 g, 4.9 mmol) was dissolved in CH_2Cl_2 (30 mL). HATU (2.00 g, 5.26 mmol), Fmoc-L-Tyr(*t*-Bu)-OH (2.48 g, 5.40 mmol), and DIEA (1.80 mL, 10.35 mmol) were added. The reaction mixture was stirred at room temperature overnight. Water and EtOAc were added, and the layers were separated. The aqueous layer was extracted with EtOAc, and the combined organic layers were washed with 1 M $KHSO_4$, water, saturated $NaHCO_3$, and brine, dried over Na_2SO_4, and evaporated. The residue was purified by column chromatography (EtOAc/pentane, 1:4) to give the Fmoc-protected amine as a white foam (4.23 g, 95%). Anal. ($C_{53}H_{56}ClN_3O_7Si$) C, H, N. DBU (0.770 mL, 5.15 mmol) was added to a solution of the Fmoc-protected amine (3.90 g, 4.28 mmol) in 25 mL of THF. After 2 h at room temperature, the reaction was completed according to TLC (2% MeOH in CH_2Cl_2). The MeOH was evaporated, and the crude product purified by column chromatography (gradient CH_2Cl_2 to 2% MeOH in CH_2Cl_2) to give the deprotected amine **14a** (2.81 g, 95%). $[\alpha]^{23}_D$ = +19° (c = 1.00, MeOH). Anal. ($C_{38}H_{46}ClN_3O_5Si$) C, H, N.

(2S)-2-(4-*tert*-Butoxybenzyl)-4-[2-(*tert*-butyldiphenylsilanyloxy)ethyl]-9-nitro-1,2,4,5-tetrahydrobenzo[1,4]-diazepin-3-one, 15a. The amine **14a** (2.60 g, 3.78 mmol) was dissolved in 30 mL of DMSO, and Et_3N (0.77 mL, 5.5 mmol) was added. The reaction mixture was heated to 100 °C and stirred for 24 h. EtOAc, water, and $NaHCO_3$ were added, and the layers were separated. The aqueous layer was extracted with EtOAc, and the combined organic layers were washed with water and brine, dried over Na_2SO_4, and evaporated. The residue was purified through column chromatography (CH_2Cl_2), and the product **15a** was obtained as a yellow foam (2.03 g, 82%). $[\alpha]^{23}_D$ = −109° (c = 1.03, MeOH). Anal. ($C_{38}H_{45}N_3O_5Si$) C, H, N.

(2S)-2-(4-*tert*-Butoxybenzyl)-4-[2-hydroxyethyl]-9-nitro-1,2,4,5-tetrahydrobenzo[1,4]diazepin-3-one, 16a. TBAF (1 M solution in THF, 3.40 mL, 3.4 mmol) was added to **15a** (1.85 g, 2.84 mmol) in THF (40 mL). After 1.5 h water and EtOAc were added, the layers were separated, and the aqueous layer was extracted with EtOAc. The combined organic layers were washed with water and brine, dried over Na_2SO_4, and evaporated. Column chromatography (1% MeOH in CH_2Cl_2) gave **15a** as a yellow foam (1.05 g, 89%). $[\alpha]^{23}_D$ = −201° (c = 1.06, MeOH). ^{1}H NMR ($CDCl_3$) δ: 8.41 (d, J = 2.8 Hz, 1H, NH), 8.04 (m, 1H, CH), 7.27 (m, 2H, 2 × CH), 7.12 (m, 1H, CH), 6.98 (m, 2H, 2 × CH), 6.52 (m, 1H, CH), 5.44 (d, J = 16.7 Hz, 1H, CH_2), 5.10 (m, 1H, CH), 3.96 (d, J = 16.7 Hz, 1H, CH_2), 3.88−3.73 (m, 3H, CH_2 and CH_2), 3.62−3.50 (m, 1H, CH_2), 3.40 (dd, J = 4.4, 14.6 Hz, 1H, CH_2), 2.94 (dd, J = 9.6, 14.6 Hz, 1H, CH_2), 2.26 (br s, 1H, OH), 1.33 (s, 9H, 3 × CH_3). ^{13}C NMR ($CDCl_3$) δ: 169.8 (C), 154.5 (C), 144.0 (C), 135.8 (CH), 133.0 (C), 131.1 (C), 129.9 (CH), 127.3 (CH), 124.5 (CH), 122.6 (C), 115.3 (CH), 78.5 (C), 61.7 (CH_2), 56.4 (CH), 53.0 (CH_2), 50.2 (CH_2), 36.7 (CH_2), 28.8 (CH_3). Anal. ($C_{22}H_{27}N_3O_5$) C, H, N.

[(2S)-2-(4-*tert*-Butoxybenzyl)-9-nitro-3-oxo-1,2,3,5-tetrahydrobenzo[1,4]diazepin-4-yl]-acetic Acid, 17a. A solution of oxalyl chloride (300 μL, 3.50 mmol) in 16 mL of CH_2Cl_2 was cooled to −78 °C. DMSO (525 μL, 7.40 mmol) was added dropwise, and the mixture was stirred for 15 min before a solution of **16a** (1.148 g, 2.78 mmol) in 5.0 mL of CH_2Cl_2 was added dropwise over 15 min. After another 2 h at −78 °C, Et_3N (1.60 mL, 11.48 mmol) was added, and the reaction mixture was allowed to warm to −30 °C over 1 h. Water (2 mL) was added to quench the reaction. The layers were separated, and the aqueous layer was extracted with CH_2Cl_2. The combined organic layers were washed with 1 M $KHSO_4$, water, saturated $NaHCO_3$ solution and brine, dried (Na_2SO_4), and evaporated. The aldehyde was obtained as an orange foam (1.03 g, 90%). $[\alpha]^{23}_D$ = −170° (c = 1.02, MeOH). ^{1}H NMR ($CDCl_3$) δ: 9.60 (s, 1H, CH), 8.43 (d, J = 2.9 Hz, 1H, NH), 8.05 (dd, J = 8.7, 1.7 Hz, 1H, CH), 7.27 (m, 2H, 2 × CH), 7.07 (dd, J = 7.1, 1.7 Hz, 1H, CH), 6.98 (m, 1H, 2 × CH), 6.54 (dd, J = 8.7, 7.1 Hz, 1H, CH), 5.58 (d, J = 16.5 Hz, 1H, CH_2), 5.17 (m, 1H, CH), 4.67 (d, J = 18.5 Hz, 1H, CH_2), 4.15 (d, J = 18.5 Hz, 1H, CH_2), 3.75 (d, J = 16.5 Hz, 1H, CH_2), 3.40 (dd, J = 14.6, 4.5 Hz, 1H, CH_2), 2.96 (dd, J = 14.6, 9.6 Hz, 1H, CH_2), 1.33 (s, 9H, 3 × CH_3). ^{13}C NMR ($CDCl_3$) δ: 196.3 (C), 169.5 (C), 154.6 (C), 143.9 (C), 135.7 (CH), 133.2 (C), 130.9 (C), 129.9 (CH), 127.5 (CH), 124.5 (CH), 121.9 (C), 115.4 (CH), 78.5 (C), 56.8 (CH_2), 56.0 (CH), 52.9 (CH_2), 36.5 (CH_2), 28.8 (CH_3). Anal. ($C_{22}H_{25}N_3O_5\cdot0.5H_2O$) C, H, N.

The obtained aldehyde was dissolved in 25 mL of *t*-BuOH and cyclohexene (4.70 mL, 46.2 mmol). The solution was cooled on an ice bath, and a freshly prepared ice-cold solution of $NaClO_2$ (2.62 g, 80%, 23.2 mmol) and $NaH_2PO_4\cdot H_2O$ (2.55 g, 18.6 mmol) in 15 mL of water was added dropwise over 10 min. After 2 h at 0 °C, the reaction was complete according to TLC (20% MeOH in CH_2Cl_2). EtOAc and water were added, and the layers were separated. The organic layer was washed with brine, dried (Na_2SO_4), and evaporated. After purification by column chromatography (gradient CH_2Cl_2 to 30% MeOH in CH_2Cl_2) the product was redissolved in EtOAc. The EtOAc solution was washed with 0.5 M $KHSO_4$, dried over Na_2SO_4, and evaporated to give **17a** as a yellow foam (947 mg, 96%). $[\alpha]^{23}_D$ = −173° (c = 1.02, MeOH). ^{1}H NMR (CD_3OD) δ: 7.91 (dd, J = 8.7, 1.6 Hz, 1H, CH), 7.32 (m, 2H, 2 × CH), 7.23 (dd, J = 7.1, 1.7 Hz, 1H, CH), 6.96 (m, 2H, 2 × CH), 6.51 (dd, J = 8.7, 7.1 Hz, 1H, CH), 5.62 (d, J = 16.6 Hz, 1H, CH_2), 5.38 (dd, J = 9.9, 4.6 Hz, 1H, CH), 4.40 (d, J = 17.5 Hz, 1H, CH_2), 4.13 (d, J = 17.5 Hz, 1H, CH_2), 4.08 (d, J = 16.6 Hz, 1H, CH_2), 3.32 (dd, J = 14.5, 4.6 Hz, 1H, CH_2), 2.90 (dd, J = 14.5, 9.9 Hz, 1H, CH_2), 1.30 (s, 9H, 3 × CH_3). ^{13}C NMR (CD_3OD) δ: 172.5 (C), 172.2 (C), 155.7 (C), 145.3 (C), 137.5 (CH), 134.2 (C), 133.2 (C), 131.3 (CH), 127.8 (CH), 125.7 (CH), 124.6 (C), 116.7 (CH), 79.8 (C), 56.8 (CH), 53.5 (CH_2), 49.6 (CH_2), 37.4 (CH_2), 29.3 (CH_3). Anal. ($C_{22}H_{25}N_3O_6\cdot0.6H_2O$) C, H, N.

[(2S)-2-(4-*tert*-Butoxybenzyl)-9-[(9*H*-fluoren-9-ylmethoxycarbonyl)amino]-3-oxo-1,2,3,5-tetrahydrobenzo[1,4]-diazepin-4-yl]-acetic Acid, 18a. HCO_2NH_4 (450 mg, 7.14 mmol) was added to a mixture of Pd/C (45 mg 10%, 42 μmol) and **17a** (203 mg, 0.47 mmol) in MeOH (7 mL). The reaction was performed under nitrogen in a sealed tube and was complete within 2.5 h. The Pd/C was removed by filtration. After evaporation, the crude product was dissolved in EtOAc and washed with water and brine. The organic layer was dried over Na_2SO_4 and evaporated. The residue was suspended in dioxane (5 mL) and cooled to 0 °C. FmocCl (182 mg, 0.70 mmol) was added, followed by the dropwise addition of 4.7 mL of 10% aqueous Na_2CO_3 at a pH of 8−9. After 48 h, diethyl ether and water were added. The layers were separated, and the aqueous layer (with a precipitate) was washed with diethyl ether until TLC showed that all impurities with R_f values higher than that of the product had been removed. More diethyl ether was added to the aqueous layer, which was acidified to pH 3 using 10% citric acid. The layers were separated, and the aqueous layer was extracted with diethyl ether. The combined organic layers were washed with water, dried (Na_2SO_4), and evaporated to give **18a** as a yellow foam (197 mg, 68%). $[\alpha]^{23}_D$ = −28° (c = 1.01, MeOH). ^{1}H NMR (CD_3OD) δ: 7.90−7.60 (m, 4H, 4 × CH), 7.48−7.21 (m, 4H, 4 × CH), 7.10 (m, 2H, 2 × CH), 7.02 (m, 1H, CH), 6.86 (m, 1H, CH), 6.59 (m, 1H, CH), 5.44 (d, J = 16.5 Hz, 1H, CH_2), 4.91 (m, 1H, CH), 4.48 (d, J =

17.4 Hz, 1H, CH_2), 4.44 (m, 1H, CH), 4.19 (m, 2H, CH_2), 4.03 (d, J = 16.5 Hz, 1H, CH_2), 3.97 (d, J = 17.4 Hz, 1H, CH_2), 3.29 (dd, J = 14.3, 4.0 Hz, 1H, CH_2), 2.79 (dd, J = 14.3, 10.0 Hz, 1H, CH_2), 1.13 (s, 9H, 3 × CH_3). ^{13}C NMR (CD_3OD) δ: 173.9 (C), 172.8 (C), 157.3 (C), 155.3 (C), 145.6 (C), 145.2 (C), 142.8 (C), 133.9 (C), 130.9 (CH), 129.0 (CH), 128.6 (CH), 128.3 (CH), 127.7 (C), 126.7 (CH), 126.4 (CH), 125.6 (CH), 123.0 (C), 121.1 (CH), 119.0 (CH), 79.4 (C), 68.5 (CH_2), 57.0 (CH), 53.6 (CH_2), 50.1 (CH_2), 48.3 (CH), 37.7 (CH_2), 29.3 (CH_3). Anal. ($C_{37}H_{37}N_3O_6 \cdot 1.5H_2O$) C, H, N.

(2S,3S)-2-(2-Chloro-3-nitrobenzylamino)-3-methylpentan-1-ol, 12b. Compound **12b** was prepared from **11** (3.90 g, 21.0 mmol) and (S,S)-2-amino-3-methyl-1-pentanol (2.50 g, 21.3 mmol) as described above in the synthesis of **12a**. The reaction mixture was heated overnight before being worked up to give **12b** as a pale yellow oil (3.29 g, 55%). $[\alpha]^{23}_D$ = +20° (c = 1.03, MeOH). Anal. ($C_{13}H_{19}ClN_2O_3$) C, H, N.

[(1*S*,2*S*)-1-(*tert*-Butyldiphenylsilanyloxymethyl)-2-methylbutyl]-(2-chloro-3-nitrobenzyl)amine, 13b. Compound **13b** was prepared from **12b** (1.40 g, 4.88 mmol) as described above for **13a**. The reaction mixture was stirred for 7 h at room temperature before the work up. Purification by column chromatography (gradient CH_2Cl_2/pentane (3:1) to CH_2Cl_2) gave **13b** as a pale yellow oil (2.17 g, 85%). $[\alpha]^{19}_D$ = +20° (c = 1.01, MeOH). Anal. ($C_{29}H_{37}ClN_2O_3Si$) C, H, N.

(2S)-2-Amino-3-(4-*tert*-butoxyphenyl)-*N*-(2-chloro-3-nitro-benzyl)-*N*-[(1S,2S)−(1-hydroxymethyl-2-methylbutyl-)]propionamide, 14b. The amine **12b** (1.75 g, 6.10 mmol) was dissolved in CH_2Cl_2 (35 mL). The solution was divided into seven process vials (5 mL each). To each vial HATU (365 mg, 0.96 mmol), Fmoc-L-Tyr(*t*-Bu)-OH (440 mg, 0.96 mmol), and DIEA (320 μL, 1.84 mmol) were added. The reaction mixtures were irradiated with microwaves at 100 °C for 15 min and were then combined and diluted with water and EtOAc. The aqueous layer was extracted with EtOAc, and the combined organic layers were washed with 1 M $KHSO_4$, water, saturated $NaHCO_3$, and brine, dried over Na_2SO_4, and evaporated. The residue was purified by column chromatography (gradient CH_2Cl_2 to 2% MeOH in CH_2Cl_2) to give the Fmoc-protected amine as a white foam (2.47 g, 56%). DBU (160 μL, 1.07 mmol) was added to a solution of the Fmoc-protected amine (650 mg, 0.89 mmol) in 6 mL of THF. After 2 h at room temperature, the MeOH was evaporated, and the product purified by column chromatography (gradient CH_2Cl_2 to 2% MeOH in CH_2Cl_2) to give the deprotected amine **14b** (370 mg, 82%). $[\alpha]^{23}_D$ = +2.5° (c = 1.03, MeOH). Anal. ($C_{26}H_{36}ClN_3O_5$) C, H, N.

(2S)-2-(4-*tert*-Butoxybenzyl)-4-[(1S,2S)−(1-hydroxymethyl-2-methyl-butyl)]-9-nitro-1,2,4,5-tetrahydrobenzo-[1,4]diazepin-3-one, 16b. Compound **16b** was prepared from **14b** (857 mg, 1.69 mmol) as described above in the synthesis of **15a**. Column chromatography (gradient CH_2Cl_2 to 2% MeOH in CH_2Cl_2) gave **16b** as a yellow foam (326 mg, 41%) and the diastereoisomer **16c** (126 mg, 16%). **16b:** $[\alpha]^{23}_D$ = −51° (c = 0.55, MeOH). ^{1}H NMR ($CDCl_3$) δ: 8.42 (d, J = 2.9 Hz, 1H, NH), 8.02 (dd, J = 8.7, 1.6 Hz, 1H, CH), 7.25 (m, 2H, 2 × CH), 7.13 (dd, J = 7.2, 1.6 Hz, 1H, CH), 6.96 (m, 2H, 2 × CH), 6.52 (dd, J = 8.7, 7.2 Hz, 1H, CH), 5.32 (d, J = 17.2 Hz, 1H, CH_2), 5.15 (m, 1H, CH), 4.38 (m, 1H, CH), 4.14 (d, J = 17.2 Hz, 1H, CH_2), 3.92 (dd, J = 11.8, 3.6 Hz, 1H, CH_2), 3.75 (dd, J = 11.8, 8.5 Hz, 1H, CH_2), 3.40 (dd, J = 14.6, 4.3 Hz, 1H, CH_2), 2.96 (dd, J = 14.6, 9.7 Hz, 1H, CH_2), 2.17 (br s, 1H, OH), 1.56 (m, 1H, CH), 1.30 (s, 9H, 3 × CH_3), 1.10 (m, 1H, CH_2), 0.90 (d, J = 6.6 Hz, 3H, CH_3), 0.86 (m, 1H, CH_2), 0.49 (t, J = 7.4 Hz, 3H, CH_3). ^{13}C NMR ($CDCl_3$) δ: 171.3 (C), 154.4 (C), 144.0 (C), 135.6 (CH), 132.9 (C), 131.4 (C), 129.9 (2 × CH), 127.1 (CH), 124.5 (2 × CH), 123.3 (C), 115.3 (CH), 78.5 (C), 62.1 (CH_2), 61.0 (CH), 56.5 (CH), 47.8 (CH_2), 36.6 (CH_2), 34.4 (CH), 28.8 (3 × CH_3), 26.0 (CH_2), 15.5 (CH_3), 10.4 (CH_3). Anal. ($C_{26}H_{35}N_3O_5 \cdot H_2O$) C, H, N. **16c:** ^{1}H NMR ($CDCl_3$) δ: 8.42 (d, J = 2.9 Hz, 1H, NH), 8.04 (m, 1H, CH), 7.27 (m, 2H, 2 × CH), 7.17 (m, 1H, CH), 6.96 (m, 2H, 2 × CH), 6.52 (m, 1H, CH), 5.27 (d, J = 16.7 Hz, 1H, CH_2), 5.10 (m, 1H, CH), 4.30 (m, 1h, CH), 4.10 (d, J = 16.7 Hz, 1H, CH_2), 3.72 (m, 2H, CH_2), 3.41 (dd, J = 14.4, 5.0 Hz, 1H, CH_2), 2.98 (dd, J = 14.4, 9.3 Hz, 1H, CH_2), 1.92 (m, 1H, CH), 1.34 (m, 1H, CH_2), 1.32 (s, 9H, 3 × CH_3), 1.05 (m, 1H, CH_2), 0.99 (d, J = 6.6 Hz, 3H, CH_3), 0.84 (t, J = 7.3 Hz, 3H, CH_3). ^{13}C NMR ($CDCl_3$) δ: 170.2 (C), 154.5 (C), 144.1 (C), 136.0 (CH), 133.0 (C), 131.4 (C), 129.9 (2 × CH), 127.2 (CH), 124.5 (2 × CH), 123.2 (C), 115.3 (CH), 78.5 (C), 62.8 (CH_2), 61.3 (CH), 56.4 (CH), 48.0 (CH_2), 36.6 (CH_2), 32.1 (CH), 28.8 (3 × CH_3), 25.8 (CH_2), 15.7 (CH_3), 10.5 (CH_3).

(2S,3S)-2-[(2S)-2-(4-*tert*-Butoxybenzyl)-9-nitro-3-oxo-1,2,3,5-tetrahydrobenzo[1,4]diazepin-4-yl]-3-methylpentanoic Acid, 17b. Compound **17b** was obtained after a two-step oxidation of **16b** (300 mg, 0.64 mmol) as described above for **17a**. Column chromatography (gradient CH_2Cl_2 to 10% MeOH in CH_2Cl_2) gave **17b** as a yellow foam (236 mg, 76%). $[\alpha]^{23}_D$ = −70° (c = 1.03, MeOH). ^{1}H NMR ($CDCl_3$) δ: 8.40 (d, J = 2.9 Hz, 1H, NH), 8.03 (dd, J = 8.7, 1.6 Hz, 1H, CH), 7.25 (m, 2H, 2 × CH), 7.16 (dd, J = 7.2, 1.6 Hz, 1H, CH), 6.97 (m, 1H, 2 × CH), 6.54 (dd, J = 8.7, 7.2 Hz, 1H, CH), 5.32 (d, J = 17.6 Hz, 1H, CH_2), 5.16−5.08 (m, 2H, 2 × CH), 4.48 (d, J = 17.6 Hz, 1H, CH_2), 3.40 (dd, J = 14.8, 4.2 Hz, 1H, CH_2), 2.96 (dd, J = 14.8, 10.1 Hz, 1H, CH_2), 1.84 (m, 1H, CH), 1.31 (s, 9H, 3 × CH_3), 1.08 (m, 1H, CH_2), 0.96 (d, J = 6.6 Hz, 3H, CH_3), 0.85 (m, 1H, CH_2), 0.52 (t, J = 7.4 Hz, 3H, CH_3). ^{13}C NMR ($CDCl_3$) δ: 174.9 (C), 170.9 (C), 154.4 (C), 143.8 (C), 135.9 (CH), 133.1 (C), 131.1 (C), 129.9 (2 × CH) 127.3 (CH), 124.5 (2 × CH), 122.9 (C), 115.6 (CH), 78.6 (C), 60.8 (CH), 56.3 (CH), 48.1 (CH_2), 36.5 (CH_2), 35.1 (CH), 28.8 (3 × CH_3), 25.4 (CH_2), 15.5 (CH_3), 10.4 (CH_3). Anal. ($C_{26}H_{33}N_3O_6$) C, H, N.

(2S,3S)-2-[(2S)-2-(4-*tert*-Butoxybenzyl)-9-[(9*H*-fluoren-9-ylmethoxycarbonyl)amino]-3-oxo-1,2,3,5-tetrahydrobenzo[1,4]diazepin-4-yl]]-3-methylpentanoic Acid, 18b. Compound **18b** was prepared from **17b** (200 mg, 0.414 mmol) as described above in the synthesis of **18a**, using Pd/C (40 mg 10%, 37 μmol) and HCO_2NH_4 (520 mg, 8.25 mmol). Dioxane (4.5 mL), FmocCl (320 mg, 1.24 mmol), and 10% Na_2CO_3 (aq) (3.6 mL) were added as described above, and the reaction was stirred at room temperature for 15 h. Extraction gave **18b** and a diastereoisomeric mixture in a ratio of ∼8:2. The crude product was purified by RP-HPLC (30 min gradient of 60−85% CH_3CN in 0.05% aqueous formic acid) to give **18b** (97 mg, 35%) as a white solid. ^{1}H NMR (CD_3OD) δ: 7.90−7.53 (m, 4H, 4 × CH), 7.50−7.17 (m, 4H, 4 × CH), 7.10 (m, 2H, 2 × CH), 7.03 (m, 1H, CH), 6.89 (m, 1H, CH), 6.65 (m, 2H, 2 × CH), 6.58 (t, J = 7.7 Hz, 1H, CH), 5.35 (m, 1H, CH_2), 4.99 (d, J = 10.7, 1H, CH), 4.45 (m, 1H, CH_2), 4.42 (m, 1H, CH), 4.32−4.00 (m, 2H, CH_2), 3.19 (dd, J = 4.3, 14.4 Hz, 1H, CH_2), 2.81 (dd, J = 10.3, 14.4 Hz, 1H, CH_2), 1.86 (m, 1H, CH), 1.16 (m, 1H, CH_2), 1.14 (s, 9H, 3 × CH_3), 0.93 (d, J = 6.6 Hz, 3H, CH_3), 0.79 (m, 1H, CH_2), 0.48 (t, J = 7.5 Hz, 3H, CH_3). ^{13}C NMR (CD_3OD) δ: 174.6 (C), 174.2 (C), 157.3 (C), 155.3 (C), 145.6 (C), 142.8 (C), 134.0 (C), 130.9 (CH), 129.0 (CH), 128.3 (CH), 127.7 (C), 126.8 (CH), 125.9 (CH), 125.6 (CH), 123.1 (C), 121.1 (CH), 119.0 (CH), 79.4 (C), 68.6 (CH_2), 62.2 (CH), 56.7 (CH), 49.9 (CH_2), 48.3 (CH), 37.6 (CH_2), 36.4 (CH), 29.3 (CH_3), 26.6 (CH_2), 16.2 (CH_3), 11.0 (CH_3). Anal. ($C_{41}H_{45}N_3O_6 \cdot H_2O$) C, H, N.

Solid-Phase Peptide Synthesis (SPPS). The peptides were synthesized manually, in 2 mL disposable syringes equipped with a porous polyetehylene filter, from His(Trt)-Pro-Phe-Wang resin[58] using standard Fmoc/*t*-Bu conditions. The Fmoc group was removed by treatment with 20% piperidine/DMF for 5 + 10 min. Coupling was achieved with PyBOP in the presence of DIEA. When templates and adjacent amino acids were coupled, prolonged reaction times were used and the completeness of the reaction was checked by PDMS or LC/MS analysis of cleaved resin samples. The Fmoc amino acids were protected as follows, Asp(O*t*-Bu), Arg(Pbf), Tyr(*t*-Bu), and His(Trt).

Ang II Analogue 3. Compound **18a** (40.0 mg, 64.5 μmol) and PyBOP (33.6 mg, 64.5 μmol) were dissolved in DMF (0.8 mL) together with DIEA (22.5 μL, 129 μmol) and allowed to react with His(Trt)-Pro-Phe-Wang resin (67.2 mg, 53.8 μmol) in a 2 mL syringe vessel for 20.5 h. PDMS analysis of a cleaved analytical sample confirmed that the coupling was complete. The resin was washed with DMF (6 × 1.5 mL, 6 × 1 min) and

the Fmoc group removed by treatment with 20% piperidine/DMF (2 × 1.5 mL, 5 + 10 min). After the sample was washed with DMF (6 × 1.5 mL, 6 × 1 min), CH_2Cl_2 (6 × 2 mL, open column), and MeOH (6 × 2 mL), the resin was dried in vacuo to give 83.3 mg.

Part of the polymer (39.6 mg, 24.3 μmol) was transferred to a second syringe and coupled in DMF (0.5 mL) with Fmoc-Val-OH (41.2 mg, 122 μmol) and PyBOP (63.2 mg, 122 μmol) in the presence of DIEA (42.3 μL, 244 μmol). PDMS analysis after 19 h showed that some unreacted material was still present on the resin. Therefore, the resin was washed with DMF (3 × 2 mL, 3 × 1 min) and the coupling was repeated in the same way for 3.5 h but with *O*-(1H-6-chlorobenzotriazol-1-yl)-1,1,3,3-tetramethyluronium tetrafluoroborate (TCTU) (43.2 mg, 122 μmol) as the activation agent. There was little improvement according to the PDMS analysis; a small amount of unreacted material still remained. The resin was washed and deprotected as described above, then washed with DMF (6 × 1.5 mL, 6 × 1 min). The desired pseudopeptide resin was produced (47.3 mg) after successive couplings of Fmoc-Arg-(Pbf)-OH (78.8 mg, 122 μmol) and Fmoc-Asp(O*t*-Bu)-OH (50.0 mg, 122 μmol) using PyBOP/DIEA activation for 2.5 h and followed by deprotection and washing with DMF, CH_2Cl_2, and MeOH.

Triethylsilane (75 μL) and 95% aq TFA (1.5 mL) were added to the partially protected peptide resin in a 3.5 mL centrifuge tube, and the mixture was agitated by rotation for 1.5 h. The polymer was removed by filtration through a small plug of glass wool in a Pasteur pipet and washed with TFA (2 × 0.3 mL). The combined filtrates were evaporated in a stream of nitrogen to 1.5 mL, and the product was precipitated with diethyl ether (12 mL). It was collected by centrifugation, washed with diethyl ether (4 × 8 mL), and dried in air and in vacuo to give 32.2 mg. LC−MS analysis showed the expected *m/z* value for the major component.

The crude material was dissolved in a mixture of H_2O (4 mL) and MeCN (0.2 mL) and purified in two runs by RP-HPLC on a 10 μm Vydac C18 column (2.2 × 25 cm) using a 60 min gradient of 5−45% MeCN in 0.1% aq TFA at a flow rate of 5 mL/min. The separation was monitored by UV absorption at 230 nm and by LC/MS and/or analytical RP-HPLC of selected fractions. The yield of the purified and lyophilized peptide was 8.0 mg (30.1%). LC/MS (M_{abs} 1092.51): 1093.7 (M + H^+), 547.6 ([M + $2H^+$]/2), 365.4 ([M + $3H^+$]/3). Amino acid analysis: Asp, 1.00; Arg, 0.95; Val, 0.48; His, 1.04; Pro, 0.98; Phe, 1.03.

Ang II Analogue 4. The second half (42.2 mg, 25.9 μmol) of the peptide resin obtained after coupling and deprotection of compound **18a** was reacted with Fmoc-Arg(Pbf)-OH (84.0 mg, 130 μmol), PyBOP (67.4 mg, 130 μmol), and DIEA (45.1 μL, 260 μmol) in DMF (0.5 mL) for 22.5 h. PDMS analysis indicated that some unreacted material still remained on the resin. The coupling, however, was not repeated since the corresponding recoupling of Fmoc-Val-OH (see above for analogue **3**) was essentially without effect. Instead, the resin was deprotected and coupled with Fmoc-Asp(O*t*-Bu)-OH (53.3 mg, 130 μmol), PyBOP (67.4 mg, 130 μmol), and DIEA (45.1 μL, 260 μmol) in DMF (0.5 mL) for 2.5 h. The Fmoc group was removed, and the polymer was washed with DMF, CH_2Cl_2, and MeOH and dried as described above. The resin (47.7 mg, 25.6 μmol) was treated with triethylsilane and 95% aq TFA for 1.5 h, and the product was precipitated and washed with diethyl ether and dried, giving 32.0 mg. LC/MS analysis showed that the material contained a considerable amount (ca 30%) of the des-Arg analogue.

The crude pseudopeptide was chromatographed in two runs on the Vydac C18 column using the same conditions as for analogue **3** above. The yield of pure lyophilized product was 5.6 mg (22.0%). LC/MS (M_{abs} 993.45): 994.6 (M + H^+), 497.9 ([M + $2H^+$]/2), 332.4 ([M + $3H^+$]/3). Amino acid analysis: Asp, 1.00; Arg, 0.33; His, 1.00; Pro, 1.00; Phe, 0.99.

Ang II Analogue 5. Compound **18a** (84.7 mg, 114 μmol) was coupled to His(Trt)-Pro-Phe-Wang resin (142 mg, 114 μmol), deprotected, washed, and dried as described above for analogue **3** to give 178 mg of product. Part of the resin (70.5 mg, 45.1 μmol) was reacted with Fmoc-Val-OH (76.5 mg, 226 μmol), PyBOP (117 mg, 226 μmol), and DIEA (78.6 μL, 452 μmol) in DMF (0.75 mL) for 16.5 h, and the coupling was repeated under the same conditions for 4 h. The polymer weighed 72.0 mg after deprotection, washing, and drying. Fmoc-Ala-OH·H_2O (36.6 mg, 111 μmol) and Fmoc-Asp(O*t*-Bu)-OH (45.7 mg, 111 μmol) were then coupled successively to an aliquot (35.5 mg, 22.2 μmol) of the resin using PyBOP/DIEA activation for 3 h. The desired, partially protected resin weighed 40.1 mg. The pseudopeptide was cleaved and deprotected by treatment with triethylsilane (50 μL) and 95% aq TFA (1.5 mL) for 2 h to give 21.2 mg of crude material. The product was dissolved in 10% MeCN (2.2 mL) and purified on a 5 μm ACE phenyl column (21.2 mm × 150 mm) using a 45 min gradient of 10−40% MeCN in 0.1% aq TFA at a flow rate of 5 mL/min. Yield: 8.0 mg (35.8%). LC/MS (M_{abs} 1007.45): 1008.7 (M + H^+), 505.1 ([M + $2H^+$]/2). Amino acid analysis: Asp, 1.01; Ala, 0.98; Val, 0.52; His, 1.00; Pro, 1.02; Phe, 0.99.

Ang II Analogue 6. A second aliquot (36.9 mg, 23.6 μmol) of the resin obtained after coupling of compound **18a** (analogue **3** above) was reacted with Fmoc-Ala-OH·H_2O (38.9 mg, 118 μmol), PyBOP (61.4 mg, 118 μmol), and DIEA (41.2 μL, 236 μmol) in DMF (0.5 mL) for 22 h. The product was washed with DMF and then the coupling was repeated for 4 h under the same conditions. The resin was deprotected and Fmoc-Asp-(O*t*-Bu)-OH (48.6 mg, 118 μmol) was coupled in the same way using a reaction time of 2.5 h. The Fmoc group was removed, and the polymer was washed and dried to give 41.0 mg. Cleavage with 95% TFA in the presence of triethylsilane afforded 23.7 mg of the crude product, which was purified on the semipreparative phenyl column as described above but with a slightly modified gradient: 5−35% MeCN in 45 min. Yield: 8.9 mg (26.6%). LC−MS (M_{abs} 908.38): 909.2 (M + H^+), 455.4 ([M + $2H^+$]/2). Amino acid analysis: Asp, 0.98; Ala, 0.28; His, 1.01; Pro, 1.02; Phe, 1.00.

Ang II Analogues 7a and 7b. Compound **18b** (43.0 mg, 63.6 μmol) was coupled to His(Trt)-Pro-Phe-2-Cl-Trityl resin (95.4 mg, 57.2 μmol) with the aid of PyBOP (33.1 mg, 63.6 μmol) and DIEA (22.2 μL, 127μmol) in DMF (1.0 mL) for 18 h. LC/MS analysis after cleavage of an analytical sample showed the reaction to be complete. The resin was washed, deprotected, and dried as above to yield 119 mg. An aliquot of the polymer (58.1 mg, 27.9 μmol) was coupled in DMF (0.5 mL) with Fmoc-Val-OH (47.5 mg, 140 μmol) using PyBOP (72.8 mg, 140 μmol) and DIEA (48.8 μL, 280 μmol) for 20 h. The reaction was incomplete according to LC−MS analysis. The coupling was repeated using the same conditions but with HATU (53.2 mg, 140 μmol) as the activating agent. The pseudo-peptide chain was further elongated by consecutive couplings with Fmoc-Arg(Pbf)-OH (90.8 mg, 140 μmol) and Fmoc-Asp(O*t*-Bu)-OH (57.6 mg, 140 μmol) using PyBOP activation for 2 h. After deprotection, the resin was washed and dried and weighed 73.5 mg. Part of the material (57.9 mg) was treated with triethylsilane (50 μL) and 95% aq TFA (1.5 mL) for 1.5 h to yield 32.6 mg of the crude product. This was dissolved in 10% MeCN (2.2 mL) and purified on the ACE phenyl column using a 60 min gradient of 15−45% MeCN in 0.1% aq TFA. Two isomers were collected. The one with the lowest retention was further purified by RP-HPLC on a 5 μm ACE CN column (21.2 mm × 50 mm) with a 30 min gradient of 5−35% MeCN in 0.1% aq TFA at a flow rate of 3 mL/min followed by rechromatography on the phenyl column. **7a**: yield, 8.4 mg (33.2%). LC/MS (M_{abs} 1148.58): 1149.3 (M + H^+), 575.3 ([M + $2H^+$]/2), 384.0 ([M + $3H^+$]/3). Amino acid analysis: Asp, 0.99; Arg, 0.99; Val, 0.49; His, 0.88; Pro, 1.01; Phe, 1.01. **7b**: yield, 1.5 mg (5.9%). LC/MS (M_{abs} 1148.58): 1149.3 (M + H^+), 575.4 ([M + $2H^+$]/2), 384.0 ([M + $3H^+$]/3). Amino acid analysis: Asp, 1.00; Arg, 0.98; Val, 0.42; His, 0.93; Pro, 1.01; Phe, 1.01.

Ang II Analogues 8a and 8b. The second half of the product obtained after coupling compound **18b** to the tripeptide resin (61.3 mg, 29.4 μmol) was reacted with Fmoc-Arg(Pbf)-OH (95.4 mg, 147 μmol), PyBOP (76.5 mg, 147 μmol), and DIEA (51.2 μL, 294 μmol) in DMF (0.5 mL) for 20 h. LC/MS analysis showed the reaction to be incomplete, and the

coupling was repeated using the same conditions but with HATU as the activating agent. Although a small amount of unreacted material still remained, the resin was deprotected and coupled with Fmoc-Asp(O*t*-Bu)-OH (60.5 mg, 147 μmol) using PyBOP/DIEA activation as above for 5 h. After the removal of the Fmoc group, the polymer was washed and dried to yield 71.1 mg. Part of the material (59.0 mg) was treated with triethylsilane (50 μL) and 95% aq TFA (1.5 mL) for 1.5 h to give 32.4 mg of the crude product. Purification was achieved by RP-HPLC on the ACE phenyl column as described for compound **7** above. **8a**: yield, 9.6 mg (37.5%). LC−MS (M_{abs} 1049.50): 1050.4 (M + H^+), 526.0 ([M + 2H^+]/2), 351.0 ([M + 3H^+]/3). Amino acid analysis: Asp, 0.99; Arg, 0.42; His, 0.88; Pro, 1.01; Phe, 1.00. Two isomers were isolated. **8b**: yield, 4.8 mg (18.7%). LC−MS (M_{abs} 1049.50): 1050.4 (M + H^+), 525.9 ([M + 2H^+]/2), 350.9 ([M + 3H^+]/3). Amino acid analysis: Asp, 0.95; Arg, 0.39; His, 0.77; Pro, 1.02; Phe, 1.03.

Rat Liver Membrane AT_1 Receptor Binding Assay. Rat liver membranes were prepared according to the method of Dudley et al.[61] Binding of [^{125}I]Ang II to membranes was conducted in a final volume of 0.5 mL containing 50 mM Tris-HCl (pH 7.4), 100 mM NaCl, 10 mM $MgCl_2$, 1 mM EDTA, 10 μM bacitracin, 10 μM pepstatin A, 10 μM bestatin, 10 μM captopril, 0.2% BSA (bovine serum albumin), liver homogenate corresponding to 5 mg of the original tissue weight, [^{125}I]Ang II (80 000 cpm, 0.03 nM), and variable concentrations (0.01 nM−1.0 μM) of test substance. The samples were incubated at 25 °C for 2 h, and binding was terminated by filtration through Whatman GF/B glass-fiber filter sheets using a Brandel cell harvester. The filters were washed with 3 × 3 mL of Tris-HCl (pH 7.4) and transferred to tubes. The radioactivity was measured in a γ-counter. Nonspecific binding was determined in the presence of 1 μM Ang II. The specific binding was determined by subtracting the nonspecific binding from the total bound [^{125}I]Ang II. IC_{50} was determined by a Scatchard analysis of data obtained with Ang II by using GraFit (Erithacus Software, U.K.). The apparent dissociation constants K_i were calculated from IC_{50} values using the Cheng−Prusoff equation[81] (K_d = 1.7 ± 0.1 nM, [L] = 0.057 nM). The binding data were best fitted with a one-site fit. All of the experiments were performed in triplicate.

Pig Myometrial Membrane AT_2 Receptor Binding Assay. Myometrial membranes were prepared from porcine uteri according to the method of Nielsen et al.[62] Potential interference by binding to AT_1 receptors was blocked by the addition of 1 μM losartan. Binding of [^{125}I]Ang II to membranes was conducted in a final volume of 0.5 mL containing 50 mM Tris-HCl (pH 7.4), 100 mM NaCl, 10 mM $MgCl_2$, 1 mM EDTA, 10 μM bacitracin, 10 μM pepstatin A, 10 μM bestatin, 10 μM captopril, 0.2% BSA, homogenate corresponding to 10 mg of the original tissue weight, [^{125}I]Ang II (80 000 cpm, 0.03 mM), and variable concentrations (0.01 nM−1.0 μM) of the test substance. Samples were incubated at 25 °C for 1.5 h and binding was terminated by filtration through Whatman GF/B glass-fiber filter sheets using a Brandel cell harvester. The filters were washed with 3 × 3 mL of Tris-HCl (pH 7.4) and transferred to tubes. The radioactivity was measured in a γ-counter. Nonspecific binding was determined in the presence of 1 μM Ang II. The specific binding was determined by subtracting the nonspecific binding from the total bound [^{125}I]-Ang II. IC_{50} was determined by a Scatchard analysis of data obtained with Ang II by using GraFit (Erithacus Software, U.K.). The apparent dissociation constants K_i were calculated using the Cheng−Prusoff equation[81] (K_d = 0.7 ± 0.1 nM, [L] = 0.057 nM). The binding data were best fitted with a one-site fit. All of the experiments were performed in triplicate.

In Vitro Morphological Effects. (A) General. The chemicals used in the present study were obtained from the following sources: Dulbecco's modified Eagle's medium (DMEM), fetal bovine serum (FBS), HAT supplement (Hypoxanthine, Aminopterin, Thymidine), and gentamycin from Gibco BRL (Burlington, ON, Canada); [Val^5]-angiotensin II from Bachem (Marina Delphen, CA); PD123,319 from RBI (Natick, MA); LY-83,583 and KT 5823 from Calbiochem-Novabiochem (La Jolla, CA); PD98,059, anti-phosphorylated p42/p44^{mapk}, and total p42/p44^{mapk} antibodies from the New England Biolabs (Beverly, MA); horseradish peroxidase-conjugated anti-mouse and anti-rabbit antibodies from Amersham Pharmacia Biotech Inc. (NJ); complete protease inhibitor, poly(vinylidene difluoride) (PVDF) membranes, and enhanced chemiluminescence (ECL) detection system from Roche Laboratories (Montreal, QC, Canada). All other chemicals were of grade-A purity.

(B) Cell Culture. NG108-15 cells (provided by Drs M. Emerit and M. Hamon, INSERM, U. 238, Paris, France) were cultured (passage 7 to 30) in DMEM with 10% fetal bovine serum (FBS, Gibco BRL, Burlington, ON, Canada), HAT supplement, and 50 mg/L gentamycin at 37 °C in 75 cm^2 Nunclon Delta flasks in a humidified atmosphere of 93% air and 7% CO_2, as previously described.[63] Subcultures were performed at subconfluency. Under these conditions, cells expressed only the AT_2 receptor subtype.[63,64] Cells were stimulated for periods ranging from minutes (MAPK) to 3 days (neurite elongation) (first stimulation 24 h after plating) according to the experiments. Cells were cultured for three subsequent days under these conditions. For all experiments, cells were plated at the same initial density of 4 × 10^4 cells/35 mm Petri dish. Cells were treated without (control cells) or with Ang II (100 nM) or one of the test compounds (100 nM), in the absence or in the presence of the various inhibitors to be tested: PD123,319 (1 μM), an AT_2 receptor antagonist, PD98,059 (10 μM), an inhibitor of MEK, LY-83,583 (0.5 μM), an inhibitor of soluble guanylyl cyclase or KT-5823 (1 μM), and an inhibitor of cGMP-dependent protein kinases (each introduced daily with inhibitors applied 30 min prior to Ang II or the tested pseudopeptide).

(C) Determination of Cells with Neurites. Cells were examined daily under a phase contrast microscope, and micrographs were taken after 3 days under the various experimental conditions. Cells with at least one neurite longer than a cell body were counted as positive for neurite outgrowth. At least 64 cells were counted in three independent experiments.[65]

(D) Western Blotting for p42/p44^{mapk}. After 3 days of culture, cells were washed with Hanks buffered saline (HBS) (HBS: 130 mM NaCl; 3.5 mM KCl; 2.3 mM $CaCl_2 \cdot 2H_2O$; 0.98 mM $MgCl_2 \cdot 6H_2O$; 5 mM HEPES; 0.5 mM EGTA) and then incubated for 10 min with 800 μL of stabilization buffer (100 nM staurosporine, 1 mM Na_3VO_4 in HBS) and finally lysed in 25 μL of lysis buffer (50 mM HEPES pH 7.8, 100 nM staurosporine, 1 mM Na_3VO_4, 1% Triton-X100, protease inhibitors). Samples were separated on 10% SDS-polyacrylamide gels. Proteins were transferred electrophoretically to PVDF membranes. Membranes were blocked with 1% gelatin, and 0.05% Tween 20 in TBS buffer (pH 7.5). After samples were washed with TBS-Tween 20 (0.05%), membranes were incubated overnight at 4 °C with antiphosphorylated p42/p44^{mapk} (1:1000) or anti-p42/p44^{mapk} (1:1000) and diluted in TBS-Tween 20 (0.05%) plus BSA (0.1%). After samples were washed with TBS-Tween 20, detection was accomplished using horseradish peroxidase-conjugated anti-mouse or anti-rabbit IgG (1:2000) and an enhanced chemiluminescence (ECL) detection system, as described previously.[23]

(E) Data Analysis. The data were presented as a mean ± standard error of mean (SEM) of the number of experiments indicated in the text, each performed in duplicate or triplicate. Statistical analyses of the data were performed using the one-way analysis of variance (ANOVA) test. Homogeneity of variance was assessed by Bartlett's test, and p values were obtained from Dunnett's tables.

Proliferation of PC12 Cells. PC12 cells, a well-characterized rat adrenal pheochromocytoma cell line, were obtained from the European Collection of Animal Cell Cultures (ECACC, Salisbury, United Kingdom). Cells were grown in suspension cultures in DMEM (Gibco-BRL, Eggenstein, Germany) with 10% fetal calf serum (FCS) in 5% CO_2 at 37 °C. PC12 cells expressed only AT_2 receptors.

Proliferation was assessed by incorporation of [^{3}H]thymidine into DNA. Cells (10^4 cells per well) were transferred to a 96-

well microtiter plate and made quiescent by incubation in serum-free medium for 12 h. Cells were then stimulated as indicated for 24 h in 10% FCS in the presence of 10^{-6} M Ang II (Sigma), 10^{-6} M PD123,319 (Sigma), or 10^{-6} M compound **1** and were pulsed with 1 μCi [^{3}H]thymidine (5 Ci/mmol, Amersham) during the last 6 h of culture. At the end of the incubation period, cells were collected on glass-fiber paper with an automatic cell harvester. Radioactivity of dry filters was measured by liquid scintillation spectroscopy. All experiments were independently performed with 10−12 replicates. All of the values are presented as means ± SEM. Statistical significance among multiple groups was first tested with the nonparametric Kruskal−Wallis test. Individual groups were then tested using the Wilcoxon−Mann−Whitney test. A p value of <0.05 was considered significant.

Conformational Analysis and Molecular Modeling. (A) **General Protocol for Conformational Analysis**. Conformational analysis was performed in MacroModel 8.5[69] using the MMFFs force field and the general Born solvent accessible (GB/SA) surface area method for water developed by Still et al.[70] Amide bonds were fixed in the trans configuration, and the number of torsion angles allowed to vary simultaneously during each Monte Carlo step ranged from 1 to $n - 1$. The ring closure bond was defined as the bond between N and C_α of the Ala residue in the model compounds. The conformational search was conducted using the systematic unbound multiple minimum (SUMM) search method[82] in the BatchMin program. Truncated Newton conjugate gradient (TNCG) minimization with a maximum of 500 iterations was used in the conformational search. Torsional memory and geometric preoptimization were used. Conformations within 5 kcal/mol of the lowest energy minimum were kept.

(B) C_α Distance Comparisons in γ-Turn Mimetics. Conformational analysis using the general protocol was performed on model compounds of scaffold **20** and **21** where tyrosine was substituted for alanine. One thousand search steps were used, and for the minimization the derivative convergence criterion was set to 0.001 kJ mol^{-1} Å^{-1}.

The distances and angles between the C_α atoms in the identified conformations were measured and compared to those in an inverse γ-turn. In this comparison, the aromatic carbon of the benzene ring in **20** and **21** that is bound to methylamide was defined as $C_{\alpha i}$. The ideal inverse γ-turn was generated by minimizing (MMFFs) a trialanine sequence with Φ_{i+1} adjusted to −77° and Ψ_{i+1} adjusted to 65° prior to the minimization.

(C) Comparison of 21 to γ-Turns in Protein Crystal Structures. The three conformations identified within 1 kcal/mol of the lowest found minimum of the model compound of **21** were compared to 2101 inverse γ-turns (defined as having torsion angles ±30° from the ideal values of residue $i + 1$), extracted from a representative set of crystallized proteins selected using the PDB_SELECT list from December 2003.[83,84] The comparison was performed by calculating the root mean square distance between the torsion angles Φ_i, Ψ_i, Φ_{i+1}, Ψ_{i+1}, Φ_{i+2}, and Ψ_{i+2} in the protein turns and the corresponding torsion angles in **21**.

(D) DISCOtech Analysis. The conformational search was performed on structures **1m**, **2m**, **3m**, and **4m** using the general protocol. For the minimization the derivative convergence criterion was set to 0.05 kJ mol^{-1} Å^{-1} and 5000 search steps per rotatable bond were used. To reduce the number of identified conformations, all folded conformations which have intramolecular hydrogen bonds with a distance of 4 Å or less between the carbon in the guanidino group and any of the carbonyl oxygens were removed. The number of conformations was reduced further in a subsequent minimization of the found conformations by increasing the convergence criteria to 0.001 kJ mol^{-1} Å^{-1} and using only four key atoms (see Figure 9) as comparison atoms (COMP). In this minimization, the criterion for a unique conformation was changed from the default maximum distance of 0.25 Å between the compared atoms after superposition (CRMS) to 0.75 Å for the analogues without valine and to 1.5 Å for the analogues with valine. Conformations within 5 kcal/mol of the lowest energy minimum were saved.

The DISCOtech[68] module in Sybyl 6.9[85] for Linux was used to find an alignment of interesting features among the conformations. Extra features were added to the molecules in DISCOtech by transforming relevant atoms of the molecules into DISCOtech recognizable features. C_β of Ala (corresponding to C_β in Tyr) was transformed into a quaternary nitrogen (DISCOtech NP feature), and the CH_3 carbon of the acetyl capping group (corresponding to C_α in Asp) and the carbon of the N−CH_3 group (corresponding to C_α in Gly) were transformed into *tert*-butyl groups (DISCOtech HY features). These features plus the acceptor sites (DISCOtech AS features) originating from the guanidino group were used in the analysis. To simplify the analysis, all atoms not included in a feature were transformed into hydrogen atoms. In this transformation, only the atom types were changed but not the geometry. The conformations from the conformational analysis of **1m** (212), **3m** (158), and **4m** (167) were imported to DISCOtech. The DISCOtech setting "Features by Class" was used to search for models containing more than zero acceptor sites (receptor points corresponding to the guanidino group), exactly two hydrophobic features (C_α of the Gly and Asp residue), and exactly one positive nitrogen (C_β of the Tyr residue). The tolerance for a feature match between the three molecules was set to start at 0.25 Å and increased in increments of 0.25 Å up to 2.5 Å if necessary. Compound **3m**, with the lowest number of identified conformations, was used as the reference molecule. The total volume of the models was calculated using the spreadsheet function Autofill (molprop_volume) in Sybyl. The same setup was used in the DISCOtech analysis when the inactive **2m** was also included (237 conformations of **2m** was used).

Acknowledgment. We gratefully acknowledge support from the Swedish Research Council, the Swedish Foundation for Strategic Research, and the Canadian Institutes of Health Research to N.G.P. (MOP 37891). N.G.P. is a holder of a Canada Research Chair in Endocrinology of the Adrenal Gland.

Supporting Information Available: ^{1}H and ^{13}C NMR spectral data of (2-chloro-3-nitrophenyl)methanol and compounds **11**, **12a**, **13a**, **14a**, **15a**, **12b**, **13b,** and **14b** and elemental analysis for all new compounds. This material is available free of charge via the Internet at http://pubs.acs.org.

References

(1) Kambayashi, Y.; Bardhan, S.; Takahashi, K.; Tsuzuki, S.; Inui, H.; Hamakubo, T.; Inagami, T. Molecular cloning of a novel angiotensin II receptor isoform involved in phosphotyrosine phosphatase inhibition. *J. Biol. Chem.* **1993**, *268*, 24543−24546.
(2) Mukoyama, M.; Nakajima, M.; Horiuchi, M.; Sasamura, H.; Pratt, R. E.; Dzau, V. J. Expression cloning of type 2 angiotensin II receptor reveals a unique class of seven-transmembrane receptors. *J. Biol. Chem.* **1993**, *268*, 24539−24542.
(3) Timmermans, P. B. M. W. M.; Wong, P. C.; Chiu, A. T.; Herblin, W. F.; Benfield, P.; Carini, D. J.; Lee, R. J.; Wexler, R. R.; Saye, J. A. M.; Smith, R. D. Angiotensin II receptors and angiotensin II receptor antagonists. *Pharm. Rev.* **1993**, *45*, 205−251.
(4) de Gasparo, M.; Catt, K. J.; Inagami, T.; Wright, J. W.; Unger, T. International union of pharmacology. XXIII. The angiotensin II receptors. *Pharm. Rev.* **2000**, *52*, 415−472.
(5) Kaschina, E.; Unger, T. Angiotensin AT1/AT2 receptors: regulation, signaling and function. *Blood Pressure* **2003**, *12*, 70−88.
(6) Horiuchi, M. Functional aspects of angiotensin type 2 receptor. *Adv. Exp. Med. Biol.* **1996**, *396*, 217−224.
(7) Csikos, T.; Chung, O.; Unger, T. Receptors and their classification: focus on angiotensin II and the AT2 receptor. *J. Hum. Hypertens.* **1998**, *12*, 311−318.
(8) Gendron, L.; Payet, M. D.; Gallo-Payet, N. The angiotensin type 2 receptor of angiotensin II and neuronal differentiation: from observations to mechanisms. *J. Mol. Endocrinol.* **2003**, *31*, 359−372.
(9) Widdop, R. E.; Jones, E. S.; Hannan, R. E.; Gaspari, T. A. Angiotensin AT2 receptors: cardiovascular hope or hype? *Br. J. Pharmacol.* **2003**, *140*, 809−824.

(10) Li, X. C.; Widdop, R. E. AT2 receptor-mediated vasodilatation is unmasked by AT1 receptor blockade in conscious SHR. *Br. J. Pharmacol.* **2004**, *142*, 821−830.
(11) Grady, E. F.; Sechi, L. A.; Griffin, C. A.; Schambelan, M.; Kalinyak, J. E. Expression of AT2 receptors in the developing rat fetus. *J. Clin. Invest.* **1991**, *88*, 921−933.
(12) Tsutsumi, K.; Saavedra, J. M. Characterization and development of angiotensin II receptor subtypes (AT1 and AT2) in rat brain. *Am. J. Physiol.* **1991**, *261*, R209−R216.
(13) Ohkubo, N.; Matsubara, H.; Nozawa, Y.; Mori, Y.; Murasawa, S.; Kijima, K.; Maruyama, K.; Masaki, H.; Tsutumi, Y.; Shibazaki, Y.; Iwasaka, T.; Inada, M. Angiotensin type 2 receptors are reexpressed by cardiac fibroblasts from failing myopathic hamster hearts and inhibit cell growth and fibrillar collagen metabolism. *Circulation* **1997**, *96*, 3954−3962.
(14) Chung, O.; Unger, T. Unopposed stimulation of the angiotensin AT2 receptor in the kidney. *Nephrol., Dial., Transplant.* **1998**, *13*, 537−540.
(15) Kimura, B.; Sumners, C.; Phillips, M. I. Changes in skin angiotensin II receptors in rats during wound healing. *Biochem. Biophys. Res. Commun.* **1992**, *187*, 1083−1090.
(16) Nio, Y.; Matsubara, H.; Murasawa, S.; Kanasaki, M.; Inada, M. Regulation of gene transcription of angiotensin II receptor subtypes in myocardial infarction. *J. Clin. Invest.* **1995**, *95*, 46−54.
(17) Viswanathan, M.; Saavedra, J. M. Expression of angiotensin II AT2 receptors in the rat skin during experimental wound healing. *Peptides* **1992**, *13*, 783−786.
(18) Nakajima, M.; Hutchinson, H. G.; Fujinaga, M.; Hayashida, W.; Morishita, R.; Zhang, L.; Horiuchi, M.; Pratt, R. E.; Dzau, V. J. The angiotensin II type 2 (AT2) receptor antagonizes the growth effects of the AT1 receptor: gain-of-function study using gene transfer. *Proc. Natl. Acad. Sci. U.S.A.* **1995**, *92*, 10663−10667.
(19) Horiuchi, M.; Akishita, M.; Dzau, V. J. Recent progress in angiotensin II type 2 receptor research in the cardiovascular system. *Hypertension* **1999**, *33*, 613−621.
(20) Nouet, S. S.; Nahmias, C. C. Signal transduction from the angiotensin II AT_2 receptor. *Trends Endocrin. Metab.* **2000**, *11*, 1−6.
(21) Inagami, T.; Kambayashi, Y.; Ichiki, T.; Tsuzuki, S.; Eguchi, S.; Yamakawa, T. Angiotensin receptors: molecular biology and signaling. *Clin. Exp. Pharmacol. Physiol.* **1999**, *26*, 544−549.
(22) Stoll, M.; Unger, T. Angiotensin and its AT_2 receptor: new insights into an old system. *Regul. Pept.* **2001**, *99*, 175−182.
(23) Gendron, L.; Laflamme, L.; Rivard, N.; Asselin, C.; Payet, M. D.; Gallo-Payet, N. Signals from the AT_2 (angiotensin type 2) receptor of angiotensin II inhibit p21ras and activate MAPK (mitogen-activated protein kinase) to induce morphological neuronal differentiation in NG108-15 cells. *Mol. Endocrinol.* **1999**, *13*, 1615−1626.
(24) Stroth, U.; Blume, A.; Mielke, K.; Unger, T. Angiotensin AT_2 receptor stimulates ERK1 and ERK2 in quiescent but inhibits ERK in NGF-stimulated PC12W cells. *Mol. Brain Res.* **2000**, *78*, 175−180.
(25) Spear, K. L.; Brown, M. S.; Reinhard, E. J.; McMahon, E. G.; Olins, G. M.; Palomo, M. A.; Patton, D. R. Conformational restriction of angiotensin II: cyclic analogues having high potency. *J. Med. Chem.* **1990**, *33*, 1935−1940.
(26) Johannesson, P.; Lindeberg, G.; Johansson, A.; Nikiforovich, G. V.; Gogoll, A.; Synnergren, B.; Le Greves, M.; Nyberg, F.; Karlén, A.; Hallberg, A. Vinyl sulfide cyclized analogues of angiotensin II with high affinity and full agonist activity at the AT_1 receptor. *J. Med. Chem.* **2002**, *45*, 1767−1777.
(27) Lindman, S.; Lindeberg, G.; Frändeberg, P.-A.; Nyberg, F.; Karlén, A.; Hallberg, A. Effect of 3−5 monocyclizations of angiotensin II and 4-AminoPhe^6-Ang II on AT_2 receptor affinity. *Bioorg. Med. Chem.* **2003**, *11*, 2947−2954.
(28) Lindman, S.; Lindeberg, G.; Gogoll, A.; Nyberg, F.; Karlen, A.; Hallberg, A. Synthesis, receptor binding affinities and conformational properties of cyclic methylenedithioether analogues of angiotensin II. *Bioorg. Med. Chem.* **2001**, *9*, 763−772.
(29) Plucinska, K.; Kataoka, T.; Yodo, M.; Cody, W. L.; He, J. X.; Humblet, C.; Lu, G. H.; Lunney, E.; Major, T. C.; Panek, R. L.; Schelkum, P.; Skeean, R.; Marshall, G. R. Multiple binding modes for the receptor-bound conformations of cyclic AII agonists. *J. Med. Chem.* **1993**, *36*, 1902−1913.
(30) Sugg, E. E.; Dolan, C. A.; Patchett, A. A.; Chang, R. S. L.; Faust, K. A.; Lotti, V. J. Cyclic disulfide analogues of [Sar1,Ile8]-angiotensin II. In *Peptides, Chemistry, Structure Biology, Proceedings of the Eleventh American Peptide Symposium*; Rivier, J. E., Marshall, G. R., Eds.; ESCOM: Leiden, The Netherlands, 1990; pp 305−306.
(31) Zhang, W.-J.; Nikiforovich, G. V.; Perodin, J.; Richard, D. E.; Escher, E.; Marshall, G. R. Novel cyclic analogues of angiotensin II with cyclization between positions 5 and 7: conformational and biological implications. *J. Med. Chem.* **1996**, *39*, 2738−2744.
(32) Matsoukas, J. M.; Polevaya, L.; Ancans, J.; Mavromoustakos, T.; Kolocouris, A.; Roumelioti, P.; Vlahakos, D. V.; Yamdagni, R.; Wu, Q.; Moore, G. J. The design and synthesis of a potent angiotensin II cyclic analogue confirms the ring cluster receptor conformation of the hormone angiotensin II. *Bioorg. Med. Chem.* **2000**, *8*, 1−10.
(33) Johannesson, P.; Lindeberg, G.; Tong, W.; Gogoll, A.; Synnergren, B.; Nyberg, F.; Karlén, A.; Hallberg, A. Angiotensin II analogues encompassing 5,9- and 5,10-fused thiazabicycloalkane tripeptide mimetics. *J. Med. Chem.* **1999**, *42*, 4524−4537.
(34) Johannesson, P.; Lindeberg, G.; Tong, W.; Gogoll, A.; Karlén, A.; Hallberg, A. Bicyclic tripeptide mimetics with reverse turn inducing properties. *J. Med. Chem.* **1999**, *42*, 601−608.
(35) Hruby, V. J.; Balse, P. M. Conformational and topographical considerations in designing agonist peptidomimetics from peptide leads. *Curr. Med. Chem.* **2000**, *7*, 945−970.
(36) Hruby, V. J. Designing peptide receptor agonists and antagonists. *Nat. Rev. Drug Discovery* **2002**, *1*, 847−858.
(37) Samanen, J. M.; Peishoff, C. E.; Keenan, R. M.; Weinstock, J. Refinement of a molecular model of angiotensin II (AII) employed in the discovery of potent nonpeptide antagonists. *Bioorg. Med. Chem. Lett.* **1993**, *3*, 909−914.
(38) Nikiforovich, G. V.; Kao, J. L. F.; Plucinska, K.; Zhang, W. J.; Marshall, G. R. Conformational analysis of two cyclic analogues of angiotensin: implications for the biologically active conformation. *Biochemistry* **1994**, *33*, 3591−3598.
(39) Nikiforovich, G. V.; Marshall, G. R. Three-dimensional recognition requirements for angiotensin agonists: a novel solution for an old problem. *Biochem. Biophys. Res. Commun.* **1993**, *195*, 222−228.
(40) Joseph, M. P.; Maigret, B.; Scheraga, H. A. Proposals for the angiotensin II receptor-bound conformation by comparative computer modeling of AII and cyclic analogues. *Int. J. Pept. Protein Res.* **1995**, *46*, 514−526.
(41) Balodis, J.; Golbraikh, A. Conformational analysis of cyclic angiotensin II analogues. *Lett. Pept. Sci.* **1996**, *3*, 195−199.
(42) Carpenter, K. A.; Wilkes, B. C.; Schiller, P. W. The octapeptide angiotensin II adopts a well-defined structure in a phospholipid environment. *Eur. J. Biochem.* **1998**, *251*, 448−453.
(43) Polevaya, L.; Mavromoustakos, T.; Zoumboulakis, P.; Grdadolnik, S. G.; Roumelioti, P.; Giatas, N.; Mutule, I.; Keivish, T.; Vlahakos, D. V.; Iliodromitis, E. K.; Kremastinos, D. T.; Matsoukas, J. Synthesis and study of a cyclic angiotensin II antagonist analogue reveals the role of $\pi^*-\pi^*$ interactions in the C-terminal aromatic residue for agonist activity and its structure resemblance with AT_1 non-peptide antagonists. *Bioorg. Med. Chem.* **2001**, *9*, 1639−1647.
(44) Boucard, A. A.; Wilkes, B. C.; Laporte, S. A.; Escher, E.; Guillemette, G.; Leduc, R. Photolabeling identifies position 172 of the human AT1 receptor as a ligand contact point: receptor-bound angiotensin II adopts an extended structure. *Biochemistry* **2000**, *39*, 9662−9670.
(45) Schmidt, B.; Lindman, S.; Tong, W.; Lindeberg, G.; Gogoll, A.; Lai, Z.; Thornwall, M.; Synnergren, B.; Nilsson, A.; Welch, C. J.; Sohtell, M.; Westerlund, C.; Nyberg, F.; Karlen, A.; Hallberg, A. Design, synthesis, and biological activities of four angiotensin II receptor ligands with γ-turn mimetics replacing amino acid residues 3−5. *J. Med. Chem.* **1997**, *40*, 903−919.
(46) Printz, M. P.; Nemethy, G.; Bleich, H. Proposed models for angiotensin II in aqueous solution and conclusions about receptor topography. *Nature (London)* **1972**, *237*, 135−140.
(47) Lindman, S.; Lindeberg, G.; Nyberg, F.; Karlén, A.; Hallberg, A. Comparison of three γ-turn mimetic scaffolds incorporated into angiotensin II. *Bioorg. Med. Chem.* **2000**, *8*, 2375−2383.
(48) Deraët, M.; Rihakova, L.; Boucard, A.; Perodin, J.; Sauve, S.; Mathieu, A. P.; Guillemette, G.; Leduc, R.; Lavigne, P.; Escher, E. Angiotensin II is bound to both receptors AT1 and AT2, parallel to the transmembrane domains and in an extended form. *Can. J. Physiol. Pharmacol.* **2002**, *80*, 418−425.
(49) Miura, S.-I.; Karnik, S. S. Angiotensin II type 1 and type 2 receptors bind angiotensin II through different types of epitope recognition. *J. Hypertens.* **1999**, *17*, 397−404.
(50) Samanen, J.; Regoli, D. Structure−activity relationships of peptide angiotensin II receptor agonists and antagonists. In *Angiotensin II Receptors, Volume I: Molecular Biology, Biochemistry, Pharmacology and Clinical Perspectives*; Ruffolo, R. R., Jr., Ed.; CRC Press: Boca Raton, FL, 1994; pp 11−97.
(51) Bouley, R.; Perodin, J.; Plante, H.; Rihakova, L.; Bernier, S. G.; Maletinska, L.; Guillemette, G.; Escher, E. N- and C-terminal structure−activity study of angiotensin II on the angiotensin AT2 receptor. *Eur. J. Pharmacol.* **1998**, *343*, 323−331.
(52) Cody, W. L.; He, J. X.; Lunney, E. A.; Humblet, C. C.; Lu, G. H.; Panek, R. L.; Dudley, D. T. Modification of the C-terminal dipeptide of angiotensin II yielded a novel series of analogues with II (AT2) receptor selectivity. *Protein Pept. Lett.* **1996**, *3*, 107−112.

(53) Speth, R. C.; Kim, K. H. Discrimination of two angiotensin II receptor subtypes with a selective agonist analogue of angiotensin II, p-aminophenylalanine6 angiotensin II. *Biochem. Biophys. Res. Commun.* **1990**, *169*, 997−1006.
(54) Aiyar, N.; Griffin, E.; Edwards, R.; Weinstock, J.; Samanen, J.; Nambi, P. Characterization of bovine ovary angiotensin II receptors using subtype-selective antagonists. *Pharmacology* **1993**, *46*, 1−8.
(55) Samanen, J.; Aiyar, N.; Edwards, R. Modifications to angiotensin II (AII) peptide analogues that reduce AT1 receptor affinity have little to no effect upon AT2 receptor affinity. In *Peptides, Proceedings of the Thirteenth American Peptide Symposium*; Hodges, R. S., Smith, J. A., Eds.; ESCOM: Leiden, The Netherlands, 1994; pp 640−642.
(56) Rosenström, U.; Sköld, C.; Lindeberg, G.; Botros, M.; Nyberg, F.; Hallberg, A.; Karlén, A. Synthesis and AT_2 receptor binding properties of angiotensin II analogues. *J. Pept. Res.* **2004**, *64*, 194−201.
(57) Johannesson, P.; Lindeberg, G.; Erdélyi, M.; Frändeberg, P.-A.; Nyberg, F.; Karlén, A.; Hallberg, A. AT_2-selective angiotensin II analogues encompassing tyrosine functionalized 5,5-bicyclic thiazabicycloalkane dipeptide mimetics. *J. Med. Chem.* **2004**, *47*, 6009−6019.
(58) Rosenström, U.; Sköld, C.; Lindeberg, G.; Botros, M.; Nyberg, F.; Karlén, A.; Hallberg, A. A selective AT_2 receptor ligand with a γ-turn-like mimetic replacing the amino acid residues 4−5 of angiotensin II. *J. Med. Chem.* **2004**, *47*, 859−870.
(59) Marshall, G. R. Determination of the receptor bound conformation of angiotensin. *Dtsch. Apoth. Ztg.* **1986**, *126*, 2783−2786.
(60) Uenishi, J. i.; Kobayashi, N.; Komine, S.; Okadai, T.; Yonemitsu, O.; Sasaki, T.; Yamada, Y. Total synthesis of (±)-acetomycin and design of esterase-resistant analogues. *Chem. Pharm. Bull.* **1999**, *47*, 517−523.
(61) Dudley, D. T.; Panek, R. L.; Major, T. C.; Lu, G. H.; Bruns, R. F.; Klinkefus, B. A.; Hodges, J. C.; Weishaar, R. E. Subclasses of angiotensin II binding sites and their functional significance. *Mol. Pharmacol.* **1990**, *38*, 370−377.
(62) Nielsen, A. H.; Schauser, K.; Winther, H.; Dantzer, V.; Poulsen, K. Angiotensin II receptors and renin in the porcine uterus: myometrial AT2 and endometrial AT1 receptors are down-regulated during gestation. *Clin. Exp. Pharmacol. Physiol.* **1997**, *24*, 309−314.
(63) Buisson, B.; Bottari, S. P.; De Gasparo, M.; Gallo-Payet, N.; Payet, M. D. The angiotensin AT2 receptor modulates T-type calcium current in nondifferentiated NG108-15 cells. *FEBS Lett.* **1992**, *309*, 161−164.
(64) Laflamme, L.; de Gasparo, M.; Gallo, J.-M.; Payet, M. D.; Gallo-Payet, N. Angiotensin II induction of neurite outgrowth by AT2 receptors in NG108-15 cells. Effect counteracted by the AT1 receptors. *J. Biol. Chem.* **1996**, *271*, 22729−22735.
(65) Gendron, L.; Cote, F.; Payet, M. D.; Gallo-Payet, N. Nitric oxide and cyclic GMP are involved in angiotensin II AT2 receptor effects on neurite outgrowth in NG108-15 cells. *Neuroendocrinology* **2002**, *75*, 70−81.
(66) Wolf, G.; Harendza, S.; Schroeder, R.; Wenzel, U.; Zahner, G.; Butzmann, U.; Freeman, R. S.; Stahl, R. A. K. Angiotensin II's antiproliferative effects mediated through AT2-receptors depend on down-regulation of SM-20. *Lab. Invest.* **2002**, *82*, 1305−1317.
(67) Berman, H. M.; Westbrook, J.; Feng, Z.; Gilliland, G.; Bhat, T. N.; Weissig, H.; Shindyalov, I. N.; Bourne, P. E. The protein data bank. *Nucleic Acids Res.* [Online] **2000**, *28*, 235−242. http://www.pdb.org/.
(68) Martin, Y. C.; Bures, M. G.; Danaher, E. A.; DeLazzer, J.; Lico, I.; Pavlik, P. A. A fast new approach to pharmacophore mapping and its application to dopaminergic and benzodiazepine agonists. *J. Comput.-Aided Mol. Des.* **1993**, *7*, 83−102.
(69) Mohamadi, F.; Richards, N. G. J.; Guida, W. C.; Liskamp, R.; Lipton, M.; Caufield, C.; Chang, G.; Hendrickson, T.; Still, W. C. MacroModel − an integrated software system for modeling organic and bioorganic molecules using molecular mechanics. *J. Comput. Chem.* **1990**, *11*, 440−467.
(70) Still, W. C.; Tempczyk, A.; Hawley, R. C.; Hendrickson, T. Semianalytical treatment of solvation for molecular mechanics and dynamics. *J. Am. Chem. Soc.* **1990**, *112*, 6127−6129.
(71) Knowle, D.; Kurfis, J.; Gavini, N.; Pulakat, L. Role of Asp297 of the AT2 receptor in high-affinity binding to different peptide ligands. *Peptides* **2001**, *22*, 2145−2149.
(72) Heerding, J. N.; Yee, D. K.; Jacobs, S. L.; Fluharty, S. J. Mutational analysis of the angiotensin II type 2 receptor: contribution of conserved extracellular amino acids. *Regul. Pept.* **1997**, *72*, 97−103.
(73) Blankley, C. J.; Hodges, J. C.; Klutchko, S. R.; Himmelsbach, R. J.; Chucholowski, A.; Connolly, C. J.; Neergaard, S. J.; Van Nieuwenhze, M. S.; Sebastian, A.; Quin, J., III.; Essenburg, A. D.; Cohen, D. M. Synthesis and structure−activity relationships of a novel series of non-peptide angiotensin II receptor binding inhibitors specific for the AT2 subtype. *J. Med. Chem.* **1991**, *34*, 3248−3260.
(74) Whitebread, S.; Mele, M.; Kamber, B.; de Gasparo, M. Preliminary biochemical characterization of two angiotensin II receptor subtypes. *Biochem. Biophys. Res. Commun.* **1989**, *163*, 284−291.
(75) Wan, Y.; Wallinder, C.; Plouffe, B.; Beaudry, H.; Kannan, M. A.; Wu, X.; Johansson, B.; Holm, M.; Botros, M.; Karlén, A.; Pettersson, A.; Nyberg, F.; Fändriks, L.; Gallo-Payet, N.; Hallberg, A.; Alterman, M. Design, synthesis and biological evaluation of the first selective nonpeptide AT_2 receptor agonist. *J. Med. Chem.* **2004**, *47*, 5995−6008.
(76) Kivlighn, S. D.; Huckle, W. R.; Zingaro, G. J.; Rivero, R. A.; Lotti, V. J.; Chang, R. S. L.; Schorn, T. W.; Kevin, N.; Johnson, R. G., Jr. Discovery of L-162,313: a nonpeptide that mimics the biological actions of angiotensin II. *Am. J. Physiol.* **1995**, *268*, R820−R823.
(77) Perlman, S.; Schambye, H. T.; Rivero, R. A.; Greenlee, W. J.; Hjorth, S. A.; Schwartz, T. W. Non-peptide angiotensin agonist. Functional and molecular interaction with the AT1 receptor. *J. Biol. Chem.* **1995**, *270*, 1493−1496.
(78) Wan, Y.; Wallinder, C.; Johansson, B.; Holm, M.; Mahalingam, A. K.; Wu, X.; Botros, M.; Karlen, A.; Pettersson, A.; Nyberg, F.; Fäendriks, L.; Hallberg, A.; Alterman, M. First reported nonpeptide AT_1 receptor agonist (L-162,313) acts as an AT_2 receptor agonist in vivo. *J. Med. Chem.* **2004**, *47*, 1536−1546.
(79) Rovnyak, G.; Andersen, N.; Gougoutas, J.; Hedberg, A.; Kimball, S. D.; Malley, M.; Moreland, S.; Porubcan, M.; Pudzianowski, A. Studies directed toward ascertaining the active conformation of 1,4-dihydropyridine calcium entry blockers. *J. Med. Chem.* **1988**, *31*, 936−944.
(80) Ricci, A.; Martani, A.; Graziani, O.; Oliva, M. L. Benzisothiazoles. II. Oxidation and nitration. *Ann. Chim. (Rome)* **1963**, *53*, 1860−1868.
(81) Cheng, Y.-C.; Prusoff, W. H. Relationship between the inhibition constant (K_i) and the concentration of inhibitor which causes 50% inhibition (I_{50}) of an enzymic reaction. *Biochem. Pharmacol.* **1973**, *22*, 3099−3108.
(82) Goodman, J. M.; Still, W. C. An unbounded systematic search of conformational space. *J. Comput. Chem.* **1991**, *12*, 1110−1117.
(83) Hobohm, U.; Scharf, M.; Schneider, R.; Sander, C. Selection of representative protein data sets. *Protein Sci.* **1992**, *1*, 409−417.
(84) Hobohm, U.; Sander, C. Enlarged representative set of protein structures. *Protein Sci.* **1994**, *3*, 522−524.
(85) *SYBYL Molecular Modeling Software,* version 6.9; Tripos Inc.: St. Louis, MO.

JM0491492